

Gravitational waves from binaries on unbound orbits

János Majár¹, Péter Forgács^{1,2}, and Mátyás Vasúth¹

¹*MTA KFKI Research Institute for Particle and Nuclear Physics, Budapest 114, P.O.Box 49, H-1525 Hungary*

²*LMPT, CNRS-UMR 6083, Université de Tours, Parc de Grandmont, 37200 Tours, France*

(Dated: December 2, 2018)

A generalized true anomaly-type parametrization, convenient to describe both bound and open orbits of a two-body system in general relativity is introduced. A complete description of the time evolution of both the radial and of the angular equations of a binary system taking into account the first order post-newtonian (1PN) is given. The gravitational radiation field emitted by the system is computed in the 1PN approximation including higher multipole moments beyond the standard quadrupole term. The gravitational waveforms in the time domain are explicitly given up to the 1PN order for unbound orbits, but the results are also illustrated on binaries on elliptic orbits with special attention given to the effects of eccentricity.

PACS numbers:

I. INTRODUCTION

Among the significant sources of gravitational waves (GWs) for ground-based interferometers [1–4] are parabolic and hyperbolic encounters of compact objects. Similarly to eccentric binaries these sources have an analytic description which allows one to evaluate the emitted gravitational wave signal in the post-Newtonian (PN) approximation [5]. During the close encounter of black holes sufficient amount of energy can be radiated in GWs resulting in the formation of a binary system. These phenomena are analyzed in [6] with the method of perturbation of orbital elements. Close encounter type sources provide more characteristic wave signals than typical elliptic binaries, since after the first quasiparabolic burstlike signal it emits further bursts quasiperiodically, until it reaches the validity region of the elliptic description. Recent estimates show that these binary interactions can contribute significantly to the sources of forthcoming advanced gravitational wave observatories [7].

A new generation of ground-based interferometric detectors and the Laser Interferometer Space Antenna (LISA) [8, 9] increase the possibility of direct detection of GWs. The LISA project aims to install a detector system into space and extend the GW observations to the low-frequency range which is inaccessible to ground-based interferometers due to the local gravitational noise. Depending on the system parameters and initial conditions parabolic and hyperbolic encounters produce GWs in the sensitivity range of LISA, between 10^{-4} and 10^{-1} Hz, as it is indicated in our study of specific binary systems. There are two well-known sources, the Hulse-Taylor pulsar [10] and the first double pulsar system J0737-3039 [11, 12] representing unique laboratories for relativistic gravitational physics which provide GWs in the frequency range of LISA. The computations presented here can be applied to the advanced ground-based detectors, too.

The classical motion and the encounter of compact objects are usually considered in the weak field, post-Newtonian regime, where the motion of the binary system is well described by perturbed Keplerian orbits. The equations of motion and the emitted radiation of these systems are analyzed in detail in the literature. First order (1PN) contributions to the dynamical evolution for general, eccentric orbits are discussed in [13]. Moreover, the solution for the radial and angular motion in quasi-Newtonian parametric form for closed and open orbits was also presented. The contributions of 2PN effects to the periastron advance and the orbital period are given in [14], where spin-orbit contribution to the secular precession of the orbit is also analyzed. Spin and tail effects on the energy and angular momentum losses were determined in [15]. The energy and angular momentum fluxes, moreover the evolution of the orbital elements and the emitted gravitational waveform of compact binaries to 2PN order are described by [16] for eccentric orbits. Their results are expressed by the generalized quasi-Keplerian description and the eccentric anomaly parametrization for general elliptic binary orbits. Later, the PN description of binaries was extended to higher orders and the energy and angular momentum fluxes are given for inspiralling compact binaries in quasielliptical orbits at 3PN [17, 18]. Moreover, 3.5PN corrections to the acceleration for a spherically symmetric nonrotating self-gravitating star can be found, *e.g.* in [19]. The 1PN accurate frequency domain waveforms are given recently in terms of tensor spherical harmonics for eccentric nonspinning compact binaries in [20].

The main expressions for the Keplerian motion of binaries on unbound orbits have been derived by many authors in a variety of different contexts. The energy and angular momentum losses for hyperbolic encounters and the capture of particles arriving from infinity were analyzed by Hansen [21], whose work is an extension of the classical results of Peters and Mathews [22] for elliptic orbits. In [23] the gravitational waveforms and the energy spectrum from two point masses in arbitrary unbound orbits were given in the quadrupole formalism. As a result, the waveform is found to be highly peaked near the periastron for large eccentricities. Gravitational bremsstrahlung radiation has

been studied in [24] by considering stars interacting on unbound orbits for the case of large impact parameters in the postlinear formalism. This description is valid for arbitrary stellar velocities and mass ratio of the two stars. Recently, the strain amplitude and the radiation luminosity have been analyzed in [25] for binaries where the periastron distance is much larger than the Schwarzschild radius of the individual stars.

There are detailed studies of the dynamics of black holes in a stellar cluster using numerical simulations that include the effects of gravitational radiation. Cross sections for mergers resulting from gravitational radiation during two and three-body encounters for a range of binary semimajor axes and mass ratios were presented in [26] with the use of numerical techniques. In [27] fluxes of energy and angular momentum and the gravitational waveforms produced by a point particle traveling around a Schwarzschild black hole on arbitrary bound and unbound orbits are given.

In our work we consider binary systems of compact objects in which the components are assumed to have negligible rotation. Both the classical motion (i.e. ignoring radiation reaction) and the radiation field itself are described in the 1PN approximation including higher multipole moments beyond the quadrupole term. We introduce a generalized true anomaly parametrization to describe the radial motion and to express all relevant dynamical quantities in terms of it. This new definition of the radial parametrization makes a unified description of both open and closed orbits possible, i.e. the parallel discussion of the elliptic, parabolic and hyperbolic cases. Moreover, we integrate the time dependence of the generalized true anomaly parameter taking into account the relevant PN contributions, yielding a complete description of the classical motion in time of the binary. Our main results are the explicit solution of the equations of motion on the one hand and the time-domain gravitational waveforms written out in detail on the other. To facilitate the use of our expressions, the coefficients of the waveforms are given in tabular form. We also present detectable waveforms for realistic sources on eccentric orbits, by numerically integrating the time dependence of the polarization states. As an extension of our previous work [28] we investigate the emitted gravitational wave signal of close hyperbolic encounters of compact objects in detail. Our main results represent the 1PN corrections to the expressions of Turner [23]. These waveforms have a burstlike character and can be applied to improve present search algorithms for the detection of gravitational waves.

Our paper is organized as follows. In Sec. II we describe the radial motion of the binary and introduce a suitable radial parametrization, the generalized true anomaly, which is valid for all type of orbital motion, namely for the elliptic, parabolic and hyperbolic cases. We analyze the connection between the coordinate time and the parametrization in Sec. III. In Sec. IV we describe the evolution of the polar angle, Υ , in the orbital plane. In Sec. V our results are specialized for the case of circular orbits. Section VI contains our main results, where the polarization states of the emitted gravitational waves are given for circular, elliptic and open orbits. In Sec. VII time-dependent gravitational waveforms are computed for such realistic systems as the Hulse-Taylor and the J0737-3039 pulsars, as well as binaries on parabolic and hyperbolic orbits, composed of $8M_{\odot}$ and $13M_{\odot}$ masses. Section VIII contains our conclusions and some technical details are relegated to Appendix A. Appendix B contains the constant coefficients of the waveforms.

Throughout the paper we use units in which $G = c = 1$.

II. DESCRIPTION OF THE MOTION AND THE PARAMETRIZATION OF THE ORBIT

Similarly to [28] we introduce two coordinate systems for the description of the classical motion of the binary and the polarization states. The z axis of the invariant coordinate system, in which the evolution of the orbital elements and the dynamics of the binary are most conveniently described, is fixed to the direction of the total angular momentum \mathbf{L} . The calculations can be simplified if the x and y axes of this system are chosen in a way that the direction of the line of sight has the components $\mathbf{N} = (\sin \gamma, 0, \cos \gamma)$ with the constant angle γ of \mathbf{L} and \mathbf{N} . In the invariant system the separation vector $\mathbf{r} = r\mathbf{n}$ is written as $\mathbf{r} = r(\cos \Upsilon, \sin \Upsilon, 0)$, where Υ is the polar angle of the motion in the orbital plane.

The expressions for the polarization states become simpler with the description of the main vector quantities and the transverse-traceless (TT) part h_{TT}^{ij} of the radiation field in the comoving system. In this coordinate system the z and x axes are aligned with the direction of the Newtonian angular momentum $\mathbf{L}_N = \mu\mathbf{r} \times \mathbf{v}$ and the separation vector \mathbf{r} , respectively, where $\mu = m_1 m_2 / m$ is the reduced mass, $m = m_1 + m_2$ is the total mass of the binary and \mathbf{v} is the relative velocity vector. The transformation between the two systems is given by a rotation around the z axis with the angle Υ .

The true anomaly parametrization, introduced for the description of Keplerian orbits, can be generalized to the perturbed Kepler problem. The form of the parametrization is determined by the radial equation of the motion,

$$\begin{aligned} \dot{r}^2 &= \frac{2E}{\mu} + \frac{2m}{r} - \frac{L^2}{\mu^2 r^2} + (\dot{r}^2)_{PN} , \\ (\dot{r}^2)_{PN} &= 3(3\eta - 1) \frac{E^2}{\mu^2} + 2(7\eta - 6) \frac{Em}{\mu r} - 2(3\eta - 1) \frac{EL^2}{\mu^3 r^2} + (5\eta - 10) \frac{m^2}{r^2} + (-3\eta + 8) \frac{mL^2}{\mu^2 r^3} , \end{aligned} \quad (1)$$

where $\eta = \mu/m$. The total energy E and the magnitude L of the total angular momentum are constants of motion which follow from a Lagrangian description [29]. The turning points, defined by $\dot{r}^2 = 0$, are solved up to the required order,

$$\begin{aligned} r_{min}^{max} &= \frac{m\mu \pm A_0}{-2E} + \delta r_{min}^{PN}, \\ \delta r_{min}^{PN} &= (\eta - 7)\frac{m}{4} \pm (\eta + 9)\frac{m^2\mu}{8A_0} \mp (3\eta - 1)\frac{A_0}{8\mu}, \end{aligned} \quad (2)$$

where $A_0 = (m^2\mu^2 + 2EL^2/\mu)^{1/2}$ is the magnitude of the Laplace-Runge-Lenz vector. To introduce the radial parametrization which is valid for all the possible values of the total energy, first we look at the following integral:

$$\tilde{\Upsilon}(r') = \Upsilon(r)|_{r_{min}}^{r'} = \int_{r_{min}}^{r'} \frac{\dot{\Upsilon} dr}{\dot{r}}.$$

The equation for the polar angle Υ can be evaluated following the description in [28],

$$\dot{\Upsilon} = \frac{L}{\mu r^2} \left\{ 1 - \left[(1 - 3\eta)\frac{E}{\mu} + (4 - 2\eta)\frac{m}{r} \right] \right\}. \quad (3)$$

As a consequence of the definition $\tilde{\Upsilon}(r_{min}) = 0$. In the case of elliptic orbits r_{min} and r_{max} are the turning points of the radial motion, while for unbounded orbits r_{min} is the only positive root, and $r_{max} = \infty$. According to these cases the value of $\tilde{\Upsilon}(r_{max})$ is the following. For elliptic and parabolic orbits we have

$$\tilde{\Upsilon}(r_{max})|_{elliptic,parabolic} = \pi\mathcal{K},$$

where $\mathcal{K} = (1 + 3m^2\mu^2/L^2)$. In the hyperbolic case

$$\tilde{\Upsilon}(r_{max})|_{hyperbolic} = \chi_{hyp}\mathcal{K} - \frac{m\mu\sqrt{2E\mu}(\eta L^2 E - 12\mu^3 m^2 - 15LE^2)}{4LA_0^2},$$

where $\chi_{hyp} = \arccos(-m\mu/A_0)$ is the maximum value of χ for the hyperbolic motion in the Newtonian case.

To get equivalent parametrization with the results of Damour and Deruelle [13] and that of [29] our generalized true anomaly parameter χ is introduced as follows

$$\frac{dr}{d(\cos \chi)} = -\gamma r^2, \quad \chi_{min}^{max} = \tilde{\Upsilon}(r_{min}^{max})/\mathcal{K}. \quad (4)$$

The solution of the radial motion is

$$r(\chi) = r_N(\chi) + r_{PN}(\chi), \quad (5)$$

where

$$\begin{aligned} r_N(\chi) &= \frac{L^2}{\mu(\mu m + A_0 \cos \chi)} \\ r_{PN}(\chi) &= -\frac{2(6 - \eta)m^4\mu^6 + 2(10 - 3\eta)EL^2m^2\mu^3 + (1 - 3\eta)E^2L^4}{2A_0\mu^3(\mu m + A_0 \cos \chi)^2} \cos \chi - \frac{2(2 - \eta)mEL^2 + (6 - \eta)m^3\mu^3}{\mu(\mu m + A_0 \cos \chi)^2}. \end{aligned} \quad (6)$$

We note that the above solution is valid for all three types of orbits.

The relation between the generalized true anomaly parameter and the coordinate time is given by

$$\frac{dt}{d\chi} = \frac{1}{\dot{r}} \frac{dr}{d\chi} = \frac{\mu r^2}{L} \left\{ 1 - \frac{1}{2L^2} [(\eta - 13)m^2\mu^2 + (3\eta - 1)A_0^2 + (3\eta - 8)m\mu A_0 \cos \chi] \right\}. \quad (7)$$

The type of orbital motion, namely elliptic, parabolic or hyperbolic, is determined by A_0 in Eq.(5) through the value of the total energy E . For elliptic orbits the energy is negative and $m\mu > A_0$. In this case the length of the separation vector is changing periodically between the turning points and the coordinate time t is a monotonically increasing function of the true anomaly parameter. For parabolic orbits the energy is zero, $m\mu = A_0$, and $r(\chi)$ diverges at $\chi = \pi$. In this limit t also diverges since $dt/d\chi \sim r^2$. For hyperbolic orbits the energy is negative and $m\mu < A_0$. The divergence of $r(\chi)$ as the parameter approaches the value $\chi = \cos^{-1}(-m\mu/A_0)$ defines the boundary of the orbit.

Because of the fact that the formal expressions of $r(\chi)$ and $dt/d\chi$ are identical for all types of orbits the integration of the angular variables formally leads to the same expressions. The difference between the three cases arises in the evaluation of the time dependence of χ and r , which is determined by the value of A_0 .

III. THE COORDINATE TIME AND THE PARAMETER

To obtain time-domain gravitational waveforms it is necessary to express the time dependence of the true anomaly parameter χ . This time dependence, however, cannot be given analytically. The most straightforward way is the numerical integration of the differential equations, nevertheless, in the case of elliptic orbits the separation of different contributions belonging to different PN orders is highly nontrivial. As a solution of this problem first we analyze the analytic form of the inverse function $t(\chi)$ and determine a general form of the inverse function $\chi(t)$.

A. Integration of $t(\chi)$

In the leading Newtonian order the connection between the coordinate time and the parameter is governed by the relation

$$\frac{dt}{d\chi} = \frac{\mu r_N^2}{L} = \frac{L^3}{\mu(m\mu + A_0 \cos \chi)^2}.$$

The solution of this equation for elliptic orbits is

$$t = \frac{2m\mu^{3/2}}{(-2E)^{3/2}} A_{ell} + \frac{LA_0 \sin \chi}{2E(A_0 \cos \chi + m\mu)}, \quad (8)$$

where

$$A_{ell} = \text{arctg} \frac{(m\mu - A_0) \text{tg} \left(\frac{\chi}{2} \right)}{\sqrt{m^2 \mu^2 - A_0^2}}.$$

For parabolic orbits we have

$$t = \frac{L^3 \text{tg} \left(\frac{\chi}{2} \right) [\text{tg}^2 \left(\frac{\chi}{2} \right) + 3]}{6\mu^3 m^2},$$

while for hyperbolic orbits the result is

$$t = -\frac{2m\mu^{3/2}}{(2E)^{3/2}} A_{hyp} + \frac{LA_0 \sin \chi}{2E(A_0 \cos \chi + m\mu)},$$

where

$$A_{hyp} = \text{arth} \frac{(m\mu - A_0) \text{tg} \left(\frac{\chi}{2} \right)}{\sqrt{A_0^2 - m^2 \mu^2}}.$$

For a complete description the perturbative solution of the relation between the coordinate time and χ is required. Up to 1PN the corrections of $r(\chi)$ in Eq.(7) are taken into account with the neglect of higher order terms. The solution for elliptic orbits is

$$t = \frac{LA_0 \sin \chi}{2E(A_0 \cos \chi + m\mu)} - \frac{m\mu^{1/2}}{4E(-2E)^{1/2}} [4\mu + E(\eta - 15)] A_{ell} - \frac{A_0 \cos \chi [4(3\eta - 1)EL^2 + 7(1 + \eta)m^2\mu^3] + m\mu [4(2\eta + 26)EL^2 + 7(31 + 3\eta)m^2\mu^3]}{8A_0\mu^2(m\mu + A_0 \cos \chi)^2}. \quad (9)$$

For parabolic orbits we have

$$t = \frac{[(3\eta - 18)m^2\mu^2 + 2L^2] \text{tg}^2 \left(\frac{\chi}{2} \right) - [(9\eta + 6)m^2\mu^2 - 6L^2]}{12\mu^3 m^2} L \text{tg} \left(\frac{\chi}{2} \right),$$

and for hyperbolic orbits the solution is

$$t = \frac{LA_0 \sin \chi}{2E(A_0 \cos \chi + m\mu)} - \frac{m\mu^{1/2}}{4E(2E)^{1/2}} [4\mu + E(\eta - 15)] A_{hyp} - \frac{A_0 \cos \chi [4(3\eta - 1)EL^2 + 7(1 + \eta)m^2\mu^3] + m\mu [4(2\eta + 26)EL^2 + 7(31 + 3\eta)m^2\mu^3]}{8A_0\mu^2(m\mu + A_0 \cos \chi)^2}. \quad (10)$$

B. Integration of $\chi(t)$

The differential equation which determines the time dependence of the parameter χ is

$$\begin{aligned} \frac{d\chi}{dt} &= \frac{L}{\mu r^2} \left\{ 1 + \frac{1}{2L^2} [(\eta - 13)m^2\mu^2 + (3\eta - 1)A_0^2 + (3\eta - 8)m\mu A_0 \cos \chi] \right\} \\ &\approx \frac{L}{\mu r_N^2} - \frac{2Lr_{PN}}{\mu r_N^3} + \frac{1}{2L\mu r_N^2} [(\eta - 13)m^2\mu^2 + (3\eta - 1)A_0^2 + (3\eta - 8)m\mu A_0 \cos \chi] , \end{aligned} \quad (11)$$

where r_N and r_{PN} are given in Eq. (6). Since we look for the solution as $\chi(t) = \chi_N(t) + \chi_{PN}(t)$, the different corrections to the above equation has to be separated. This process can easily be done in the case of open orbits, where $\chi(t)$ is a bounded function at every PN order. In this case the differential equations for χ are

$$\begin{aligned} \frac{d\chi_N}{dt} &= \left. \left(\frac{d\chi}{dt} \right) \right|_N = \frac{\mu(\mu m + A_0 \cos \chi_N)^2}{L^3} \\ \frac{d\chi_{PN}}{dt} &= \left. \left(\frac{d\chi}{dt} \right) \right|_{PN} = -\frac{2A_0\chi_{PN} \sin \chi_N \mu(\mu m + A_0 \cos \chi_N)}{L^3} - \frac{2\mu^2(\mu m + A_0 \cos \chi_N)^3 r_{PN}(\chi_N)}{L^5} \\ &\quad + \frac{\mu(\mu m + A_0 \cos \chi_N)^2}{2L^5} [(\eta - 13)m^2\mu^2 + (3\eta - 1)A_0^2 + (3\eta - 8)m\mu A_0 \cos \chi_N] , \end{aligned} \quad (12)$$

where

$$r_{PN}(\chi_N) = -\frac{2(6 - \eta)m^4\mu^6 + 2(10 - 3\eta)EL^2m^2\mu^3 + (1 - 3\eta)E^2L^4}{2A_0\mu^3(\mu m + A_0 \cos \chi_N)^2} \cos \chi_N - \frac{2(2 - \eta)mEL^2 + (6 - \eta)m^3\mu^3}{\mu(\mu m + A_0 \cos \chi_N)^2} .$$

Since χ and χ_{PN} are bounded functions of time the equations can be integrated numerically without difficulty.

For elliptic orbits because the time dependence of χ_{PN} is given by an unbounded function, therefore simple series expansion gives rise to secular divergences. To deal with this problem one has to separate the bounded and unbounded terms in χ_N and χ_{PN} .

To find the solution we note that $t(\chi)$ can be written as

$$\begin{aligned} t(\chi) &= T\chi + f(\chi) \\ &= t_N(\chi) + t_{PN}(\chi) = (T_N + T_{PN})\chi + f_N(\chi) + f_{PN}(\chi) , \end{aligned} \quad (13)$$

where T_N and T_{PN} are constants, and the functions $f_N(\chi)$ and $f_{PN}(\chi)$ are bounded. To prepare the numerical inversion of $t(\chi)$, first we use the following general theorem about smooth functions.

Let $F(x)$ be a smooth function, which can be written in the form $y = F(x) = Ax + B(x)$, where $A \neq 0$ is constant, and $B(x)$ is a bounded function of x . If the F^{-1} inverse function exists, writing it in the form $F^{-1}(y) = y/A + b(y)$, $b(y)$ will be a bounded function of y .

With the use of this theorem we look for the solution in the following form:

$$\begin{aligned} \chi(t) &= \Omega t + g(t) \\ &= \Omega_N t + g_N(t) + \Omega_{PN} t + g_{PN}(t) . \end{aligned} \quad (14)$$

The constants T_N , T_{PN} , and hence Ω_N and Ω_{PN} can be determined by the investigation of the circular orbit limit. The results are

$$\Omega_N = \frac{(-2E)^{3/2}}{m\mu^{3/2}} , \quad \Omega_{PN} = -\frac{(\eta - 15)E^3}{(-2E)^{1/2}m\mu^{5/2}} .$$

Moreover, we note that the use of the straightforward series expansion during the calculation of the sine and cosine of $\chi(t)$ results in the appearance of secular divergences. To solve this problem, as an example, the following expression is to be used:

$$\sin \chi(t) = \sin [\Omega_N t + \Omega_{PN} t + g_N(t)] + \cos [\Omega_N t + \Omega_{PN} t + g_N(t)] g_{PN}(t) ,$$

and similarly for $\cos \chi(t)$, which leads to a combined amplitude and frequency series expansion. In our calculations we use the above expansion to avoid secular divergences in the description of the motion of the binary and the time dependence of the polarization states of the detectable waveform.

Although the above expansion helps us to avoid the appearance of secular terms, it gives rise to technical difficulties when separating the different PN corrections on the level of Eq.(11). With the integration of both the Newtonian order and the full equation, one can determine $g_N(t)$ and $g_{PN}(t)$ separately, and give the full description of the time dependence of χ . The details of the calculations are given in Appendix A.

IV. ANGULAR EVOLUTION

Similarly to r the polar angle Υ is decomposed as

$$\Upsilon = \Upsilon_N + \Upsilon_{PN} .$$

To solve the equations of motion the form of the relative velocity vector is required in terms of the Euler angles. In the invariant system it is expressed as $\mathbf{v} = (\dot{r}, r\dot{\Upsilon}, 0)$. For the description of gravitational waves and the equations of motion one needs an alternative form of the components of the velocity vector, both in their general form and in terms of the parametrization.

In terms of the constants of motion one can express \dot{r}^2 , Eq.(1), and the square of the velocity vector, which is

$$v^2 = \frac{2E}{\mu} + \frac{2m}{r} - \left[3(1-3\eta) \left(\frac{E}{\mu} \right)^2 + 2(6-7\eta) \frac{Em}{\mu r} + (10-5\eta) \left(\frac{m}{r} \right)^2 - \frac{\eta mL^2}{\mu^2 r^3} \right] .$$

From our previous results it follows that $v_{\parallel}^2 = \dot{r}^2$ and, moreover,

$$v_{\perp}^2 = v^2 - \dot{r}^2 = \frac{L^2}{\mu^2 r^2} - (2-6\eta) \frac{EL^2}{\mu^3 r^2} - (8-4\eta) \frac{mL^2}{\mu^2 r^3} .$$

This indicates that

$$v_{\perp} = \frac{L}{\mu r_N} - \frac{L}{\mu r_N} \left[\frac{r_{PN}}{r_N} + (1-3\eta) \frac{E}{\mu} + (4-2\eta) \frac{m}{r_N} \right] .$$

When we insert the parameter dependence of r_N and r_{PN} in the above formulas the components of the velocity vector become

$$v_{\parallel} = \frac{A_0 \sin \chi}{L} + \frac{2(\eta-1)m^4\mu^6 + 3(3\eta-1)E^2L^4 + 2(4\eta-5)EL^2m^2\mu^3}{2\mu^2 A_0 L^3} \sin \chi - \frac{(8-3\eta)m\mu A_0^2}{2L^3} , \quad (15)$$

and

$$v_{\perp} = \frac{\mu m + A_0 \cos \chi}{L} - \frac{2(9-10\eta)m^4\mu^6 + 2(7-8\eta)EL^2\mu^3m^2 + 3(1-3\eta)E^2L^4}{2\mu^2 A_0 L^3} \cos \chi + \quad (16)$$

$$\frac{(2+\eta)m^3\mu^3 + (3+\eta)mEL^2}{2L^3} + \frac{2(\eta-2)m^3\mu^3 + 4(\eta-2)mEL^2}{L^3} \cos^2 \chi , \quad (17)$$

From the relation $v_{\perp} = r\dot{\Upsilon}$ we have

$$\dot{\Upsilon} = \frac{L}{\mu r_N^2} \left\{ 1 - \left[\frac{2r_{PN}}{r_N} + (1-3\eta) \frac{E}{\mu} + (4-2\eta) \frac{m}{r_N} \right] \right\} , \quad (18)$$

which can be expressed in terms of the parametrization as

$$\left(\frac{d\Upsilon}{d\chi} \right) = 1 - \frac{6m^2\mu^2 + \eta m\mu A_0 \cos \chi}{2L^2} .$$

The solution for Υ is

$$\Upsilon = \Upsilon_0 + \chi - \frac{6m^2\mu^2\chi + \eta m\mu A_0 \sin \chi}{2L^2} . \quad (19)$$

The separation vector and the waveforms contain expressions of $\sin \Upsilon$ and $\cos \Upsilon$, and their higher harmonics. With the use of a series expansion, for example, $\sin \Upsilon$ can be expressed as

$$\sin \Upsilon = \sin(\Upsilon_0 + \chi) - \cos(\Upsilon_0 + \chi) \left(\frac{6m^2\mu^2\chi + \eta m\mu A_0 \sin \chi}{2L^2} \right) .$$

For elliptic orbits there is no upper limit for χ as a function of the coordinate time and the $(3m^2\mu^2/L^2)\chi \cos(\Upsilon_0 + \chi)$ perturbative term gives rise to a secular divergence. To handle this problem we follow the method described above in the case of the time dependence of the parameter, namely, instead of the above expression we apply the following decomposition:

$$\sin \Upsilon = \sin \left(\Upsilon_0 + \chi - \frac{3m^2\mu^2\chi}{L^2} \right) - \cos \left(\Upsilon_0 + \chi - \frac{3m^2\mu^2\chi}{L^2} \right) \frac{\eta m\mu A_0 \sin \chi}{2L^2} ,$$

where no linear terms appear (note that a similar expression is valid for $\cos \Upsilon$).

V. EQUATIONS OF MOTION FOR CIRCULAR ORBITS

The relative velocity vector can generally be written as $\mathbf{v} = \dot{r}\mathbf{n} + r\omega\mathbf{m}$, where \mathbf{m} is the unit vector in the direction of the y axis of the comoving system. The definition of a circular orbit is

$$\dot{r} = \dot{\omega} = 0 .$$

From the above decomposition of the relative velocity it turns out that $\omega = \dot{\Upsilon}$. As a consequence,

$$v = v_{\perp} = \frac{L}{\mu r} \left[1 - (1 - 3\eta)\frac{E}{\mu} - (4 - 2\eta)\frac{m}{r} \right] . \quad (20)$$

In the circular orbit limit the constant radius r of the orbit cannot be evaluated analytically in all orders of the approximation and hence in our calculations we keep r as a constant parameter determined later.

From Eq.(20) the time evolution of Υ can be written as

$$\Upsilon = \frac{Lt}{\mu r^2} \left[1 - (1 - 3\eta)\frac{E}{\mu} - (4 - 2\eta)\frac{m}{r} \right] . \quad (21)$$

During the evaluation of quantities including the sine and cosine of Υ there are difficulties occurring in connection with the secular divergences as in the elliptic case. The solution of this problem is the same, although it leads to simpler form. For example,

$$\sin \Upsilon = \sin \left\{ \frac{Lt}{\mu r^2} \left[1 - (1 - 3\eta)\frac{E}{\mu} - (4 - 2\eta)\frac{m}{r} \right] \right\} .$$

In this case the secular terms can be treated with a simple expansion series of the orbital frequency.

VI. THE STRUCTURE OF THE DETECTABLE WAVEFORM

The parameter and, for circular orbits, time dependence of the waveform and the polarization states h_{+} and h_{\times} are determined by the use of the method described in [28]. The polarization states of the detectable gravitational waves are calculated by the projections of the transverse-traceless tensor h_{TT}^{ij} representing metric perturbations,

$$h_{+} = \frac{1}{2}(p_i p_j - q_i q_j) h_{TT}^{ij} , \quad h_{\times} = \frac{1}{2}(p_i q_j + q_i p_j) h_{TT}^{ij} ,$$

where \mathbf{p} is a unit vector in the orbital plane perpendicular to the direction of the line of sight \mathbf{N} , and $\mathbf{q} = \mathbf{N} \times \mathbf{p}$.

Since we have chosen the comoving system to describe this projection of h_{TT}^{ij} we determine the components of \mathbf{N} , \mathbf{p} and \mathbf{q} in this system. With the use of the transformation law between the two coordinate systems \mathbf{N} has the following form in the comoving system:

$$\mathbf{N} = \begin{pmatrix} \sin \gamma \cos \Upsilon \\ -\sin \gamma \sin \Upsilon \\ \cos \gamma \end{pmatrix} .$$

Moreover, the conditions for \mathbf{p} determine its components as

$$\mathbf{p} = \begin{pmatrix} \sin \Upsilon \\ \cos \Upsilon \\ 0 \end{pmatrix} .$$

To separate the different contributions the transverse-traceless part of the radiation field h_{TT}^{ij} can be decomposed in the post-Newtonian approximation as [30]

$$h_{TT}^{ij} = \frac{2\mu}{D} [Q^{ij} + P^{0.5}Q^{ij} + PQ^{ij}]_{TT} ,$$

where D is the distance between the observer and the source and we have collected all the terms which are relevant up to 1 PN order. Q^{ij} denotes the quadrupole (or Newtonian) term, $P^{0.5}Q^{ij}$, and PQ^{ij} are higher order relativistic corrections. The detailed expressions for these contributions are given in [30, 31].

We choose a similar decomposition for the polarization states h_+ and h_\times ,

$$h_\times = \frac{2\mu}{D} \left[h^{N_\times^+} + h^{0.5_\times^+} + h^{1_\times^+} \right],$$

It is worth mentioning that this decomposition is formal in the sense that higher order terms in the description of motion can cause higher order contributions in $h^{N_\times^+}$.

Since the description of the motion of the binary system has different properties for the different types of the orbit, and hence one can use different simplifications throughout the evaluations, the elliptic, circular, and open orbit cases are discussed separately including the description of the simplifications and the structure of the detectable waveform. The constant coefficients are given in detail in Appendix B.

A. The elliptic orbit case

For elliptic orbits a combined series expansion has to be included to deal with the problem of secular divergences described above. These secular terms give rise to a frequencylike series beside the usual amplitude expansion. In order to define this we introduce

$$\chi' = \Upsilon_0 + \chi - \frac{3m^2\mu^2}{L^2}\chi, \quad (22)$$

which is valid up to 1PN. To lowest, Newtonian order the above definition becomes simply $\chi' = \Upsilon_0 + \chi$. Since our goal is to give waveform expressions valid up to 1PN in the following in our expressions the original definition of χ' will be used.

Following the main steps described above, the parameter dependence of the detectable gravitational waveform for eccentric orbits can be given as

$$\begin{aligned} h^{N_\times^+} &= \sum_{k=-2}^2 \sum_{j=-3}^3 \left[C_{k,j}^{N_\times^+} \cos(k\chi' + j\chi) + S_{k,j}^{N_\times^+} \sin(k\chi' + j\chi) \right], \\ h^{0.5_\times^+} &= \sum_{k,j=-3}^3 \left[C_{k,j}^{0.5_\times^+} \cos(k\chi' + j\chi) + S_{k,j}^{0.5_\times^+} \sin(k\chi' + j\chi) \right], \\ h^{1_\times^+} &= \sum_{k,j=-4}^4 \left[C_{k,j}^{1_\times^+} \cos(k\chi' + j\chi) + S_{k,j}^{1_\times^+} \sin(k\chi' + j\chi) \right], \end{aligned} \quad (23)$$

where the S and C coefficients are depending on the energy E , the magnitude of the total angular momentum L , the masses of the objects and the γ angle, and hence they are constants. The explicit form of these constant coefficients is given in Appendix B.

It is worth mentioning that the above expansions are formal, since the time dependence of the true anomaly parameter χ contains higher order corrections. These can modify the expressions for both the secular terms and the amplitude expansion. Completing the analysis one arrives to a combined frequency and amplitude series expansion. In this work the whole method is used to evaluate (numerically) the time dependence of the polarization states shown in the next chapter.

B. The circular orbit case

As it has been shown in the circular orbit case we use the r constant length of the separation vector as a parameter throughout our calculations. In this case Eq.(22) reduces to

$$\chi' = \Upsilon_0 + \frac{Lt}{\mu r^2} - \frac{Lt}{\mu^2 r^3} [(1 - 3\eta)Er + (4 - 2\eta)m\mu] = \Upsilon_0 + \omega_{NT}t + \omega_{PN}t.$$

With the use of this notation the structure of the detectable waveform becomes

$$\begin{aligned}
h^{N\ddagger} &= \sum_{k=0}^2 [C_k^{N\ddagger} \cos(k\chi') + S_k^{N\ddagger} \sin(k\chi')] , \\
h^{0.5\ddagger} &= \sum_{k=0}^3 [C_k^{0.5\ddagger} \cos(k\chi') + S_k^{0.5\ddagger} \sin(k\chi')] , \\
h^{1\ddagger} &= \sum_{k=0}^4 [C_k^{1\ddagger} \cos(k\chi') + S_k^{1\ddagger} \sin(k\chi')] .
\end{aligned} \tag{24}$$

Again, the S and C constant coefficients are depending on E , L , the masses, r , and the angle γ . The explicit form of these coefficients is given in Appendix B.

The high frequency terms in h^N arise from the 1PN terms of the description of motion. At the Newtonian order the frequency of the detectable waveform is twice the orbital frequency ω_N , in agreement with the quadrupole formalism.

C. Waveforms for open orbits

The evaluation process of the waveform is almost the same as it is in the elliptic case. The only difference is that there are no secular terms arising in the parabolic and hyperbolic cases, and it is possible to use the usual expansion of the sine and cosine of the angular variables. The parameter dependence of the polarization states can be written as

$$\begin{aligned}
h^{N\ddagger} &= \chi \sum_{k=0}^3 [C_{k\chi}^{N\ddagger} \cos(k\chi) + S_{k\chi}^{N\ddagger} \sin(k\chi)] + \sum_{k=0}^4 [C_k^{N\ddagger} \cos(k\chi) + S_k^{N\ddagger} \sin(k\chi)] , \\
h^{0.5\ddagger} &= \sum_{k=0}^6 [C_k^{0.5\ddagger} \cos(k\chi) + S_k^{0.5\ddagger} \sin(k\chi)] , \\
h^{1\ddagger} &= \sum_{k=0}^7 [C_k^{1\ddagger} \cos(k\chi) + S_k^{1\ddagger} \sin(k\chi)] ,
\end{aligned} \tag{25}$$

where the constant coefficients are depending on the same parameters as in the elliptic case, and, moreover, on the Υ_0 initial value of Υ . We note that the first type of terms in h^N are linear in the parameter. In these terms all the coefficients are at 1PN order, and since the value of the parameter is bounded, the description is self-consistent.

VII. REALISTIC WAVEFORM SIGNALS

Following the description above, after the integration of the time dependence of the generalized true anomaly parameter the realistic, time-dependent gravitational waveforms can be given. In this section we present Newtonian waveforms as well as 0.5PN and 1PN corrections for well-known or reference systems in order to analyze the effects of the orbital eccentricity.

A. Waveform of realistic elliptic binaries

For further investigation, we numerically integrate the time dependence of the polarization states of the detectable waveform for two realistic and well-known sources, namely, the Hulse-Taylor and J0737-3039 pulsars, see Table I. Our goal is to investigate the effects of the eccentricity of the orbit and the 0.5PN and 1PN corrections to the waveform.

Parameters	Hulse-Taylor	J0737-3039
Mass of object 1 (m_1)	1.441 M_\odot	1.337 M_\odot
Mass of object 2 (m_2)	1.387 M_\odot	1.25 M_\odot
Eccentricity (ϵ)	0.617	0.0878
Periastron (a)	$1.9501 \cdot 10^9$ [m]	$0.8787 \cdot 10^9$ [m]
Distance from detector (D)	21000 [ly]	1956 [ly]
Orbital frequency (T_{orb})	27907 [s]	8834 [s]
J-N angle (γ)	21.12°	28.89°

Table I: Parameters of the investigated sources

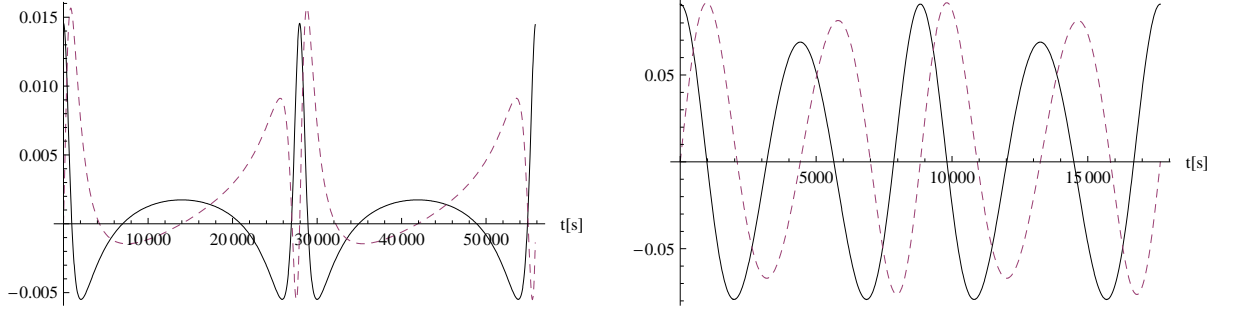


Figure 1: Time dependence of the polarization states (h_+ depicted by solid line and h_\times corresponds to dashed line) at the Newtonian order for the Hulse-Taylor (left) and for the J0737-3039 pulsars (right). The amplitudes are multiplied by the factor 10^{20} .

To keep our figures transparent, the h_+ and h_\times polarization states will be shown on the same plot. We collect the results belonging to different sources and PN orders. This simplification allows us to show the main differences between the selected systems order by order.

Following these guidelines, first we show the polarization states at the Newtonian order.

Figure 1 shows that the eccentricity of the orbit leads to many differences between the waveform predictions of the different sources. In the case of the Hulse-Taylor pulsar, the results for the emitted waveform are significantly different from the usual circular orbit case, since the eccentricity gives rise to many higher harmonics of the waveform. In the case of J0737-3039 pulsar, the eccentricity is almost 1 order of magnitude smaller and the emitted waveform is similar to the one generated by binaries on the circular orbit. We note that these differences are much more significant than the higher corrections of the PN series in both cases.

The amplitude of the emitted waveform of J0737-3039 is much higher than that of the Hulse-Taylor pulsar since the periastron of the former is less than half of the latter one, and it is much closer to the detector.

The higher order corrections show the same properties of the waveforms for the different sources. It is worth mentioning that in the circular orbit limit the frequency of the emitted waveform is twice the orbital frequency of the motion.

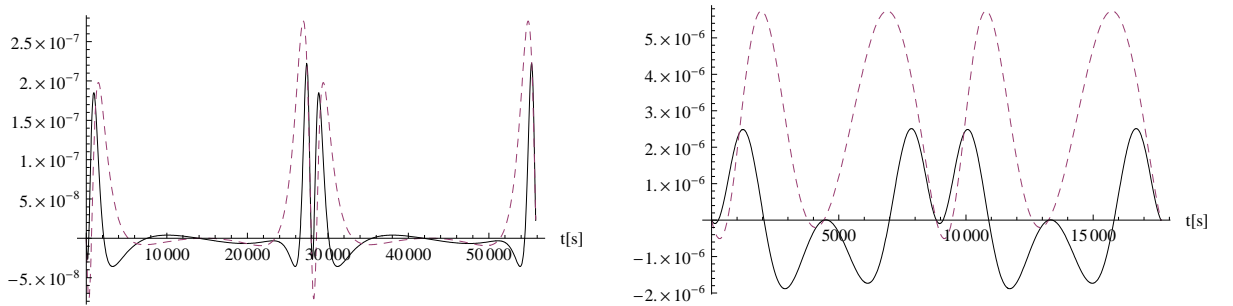


Figure 2: Time dependence of the first corrections to the polarization states at 0.5PN order. Again, h_+ is depicted by the solid line and h_\times by the dashed line. The corrections for the Hulse-Taylor pulsar are shown on the left and for the J-0737 pulsar on the right. For further comparison amplitudes are multiplied by the factor 10^{20} .

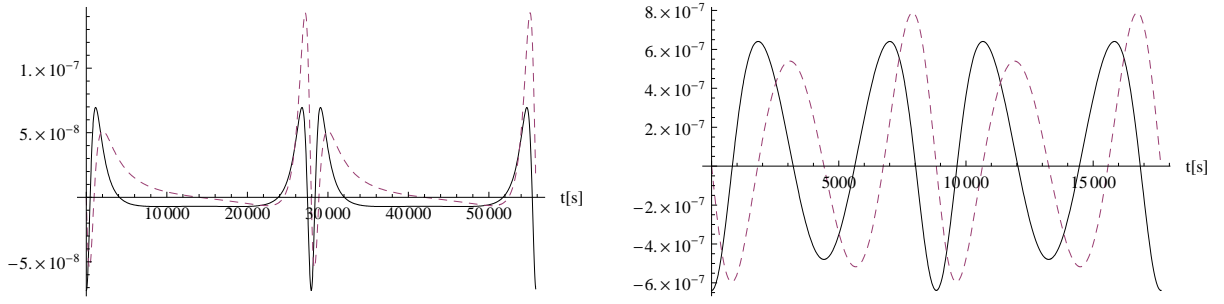


Figure 3: Multipolar corrections to the polarization states at 1PN order. Again, the corrections for the Hulse-Taylor pulsar are shown on the left, and for the J0737-3039 pulsar on the right. Solid line shows the h_+ polarization state, and dashed line shows h_\times . Again, the amplitudes are multiplied by the factor 10^{20} .

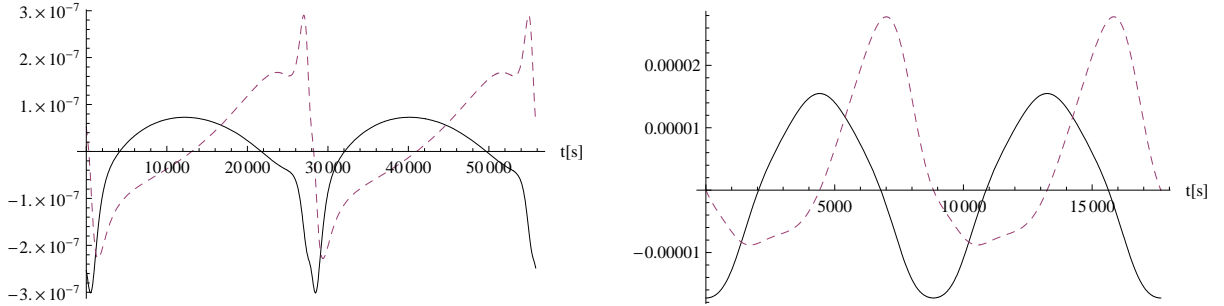


Figure 4: 1PN order corrections to the polarization states, which arise from the perturbative description of the elements of the motion. The corrections for the Hulse-Taylor pulsar are shown on the left and for the J0737-3039 pulsar on the right. The solid line shows the h_+ polarization state and the dashed line shows h_\times . To compare the different terms of these corrections, the amplitudes are multiplied by the same factor as before, namely 10^{20} .

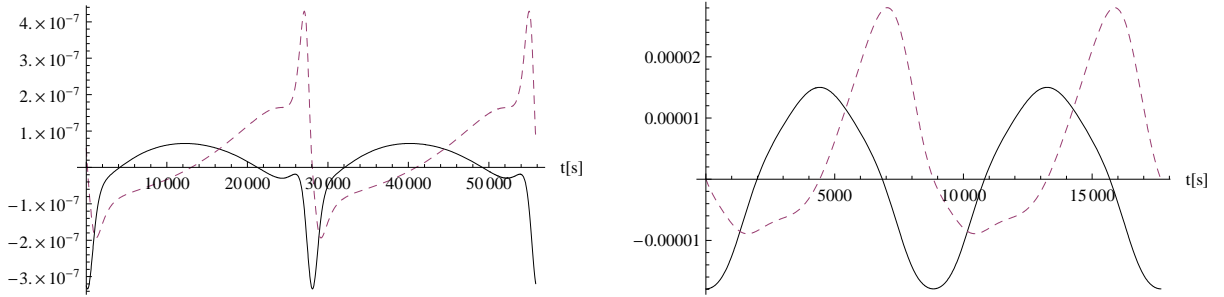


Figure 5: In these figures we plot the full 1PN corrections to the polarization states for the Hulse-Taylor pulsar (left) and for the J0737-3039 pulsar (right). The solid line represents the h_+ polarization state and the dashed line shows h_\times .

Beyond the properties described above there are two additional effects on the waveform shown by Figs. 2-5. By comparing the leading amplitudes of the different corrections it turns out that, since the masses of the objects are almost equal for both sources, and the 0.5PN order corrections are multiplied by δm , these corrections to the waveform are suppressed by the simple 1PN corrections.

Since the lowest order corrections to the dynamical variables arise at 1PN, the 0.5PN corrections to the waveform are originated only from the multipolar expansion. For 1PN corrections both the multipolar expansion and the contributions from the description of the motion contribute to the waveform. On the other hand 1PN corrections from the orbital motion of the binaries are much more significant than the contributions from the multipolar expansion of the post-Minkowskian series.

Although a full analysis of the waveform would require Fourier expansion, the main properties of these realistic waveforms are transparent. The contributions which can be seen only on long-term calculations are from the 1PN

corrections to the frequency of the waveform arising through the time dependence of true anomaly parameter and the periastron precession. These effects cause the slow shift of the basic frequency of the waveform.

B. Waveform of reference parabolic and hyperbolic orbits

Our main goal is to evaluate the first corrections to the detectable gravitational waves emitted by binaries scattering on hyperbolic and parabolic orbits.

To investigate the properties of the emitted waveforms of scattering binary systems, we introduce two hypothetical reference binaries, see Table II. The masses of the orbiting bodies are chosen following the parameter estimations in [7], although we determined the values in a way which avoids the suppression of the 0.5PN corrections. The minimal distance between the objects and the distance from the detector are chosen to be the same as in the case of the Hulse-Taylor pulsar. It will give the opportunity to compare the waveform properties between open and closed orbits.

To investigate sources in which the emission of GWs results in the formation of a closed binary (in extreme cases even zoom-whirl orbits) we discuss parabolic sources. To analyze the effects of the eccentricity, besides parabolic orbits we introduce a hyperbolic source ($\epsilon = 2$).

Parameters	Hypothetic sources
Mass of object 1 (m_1)	8 M_\odot
Mass of object 2 (m_2)	13 M_\odot
Eccentricity (ϵ)	1 and 2
Minimal distance (r_{min})	$1.9501 \cdot 10^9$ [m]
Distance from detector (D)	21000 [ly]
J-N angle (γ)	45°

Table II: Parameters of the investigated open sources

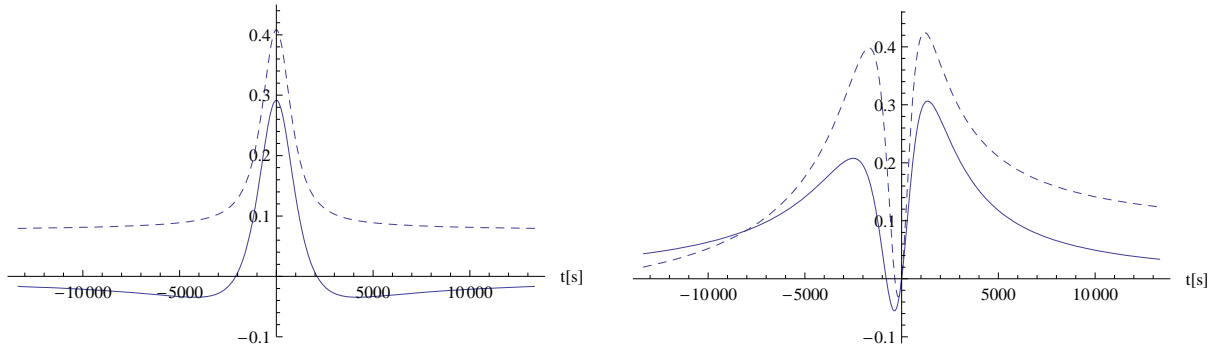


Figure 6: Time dependence of the polarization states at Newtonian order for the two open orbit sources. The solid line shows the parabolic case and the dashed line shows the waveform of the hyperbolic ($\epsilon = 2$) source. The h_+ polarization state are depicted on the left figure and h_\times is shown on the right one. The amplitudes are multiplied by the factor 10^{20} .

The waveform for open orbits is not periodic (or quasiperiodic), it is burstlike, as it is shown in [23]. Our hypothetical sources provide a high amplitude signal in the scale of a few hours. Binaries in [7] provide gravitational waves with higher amplitude, since the minimal distance between the objects are much smaller than ours.

In Figs. 6-10, it can be seen that the eccentricity of the orbit affects the frequency of the emitted signal. With the same properties, the higher the eccentricity, the more spiky the signal with higher amplitude at each PN order.

VIII. CONCLUDING REMARKS

We have introduced a generalized true anomaly parametrization for binary systems on either closed or on open orbit and applied it to evaluate gravitational waveforms emitted by them. In addition to elliptic orbits we consider the scattering of binary systems following quasiparabolic and quasihyperbolic orbits. Our new parametrization leads

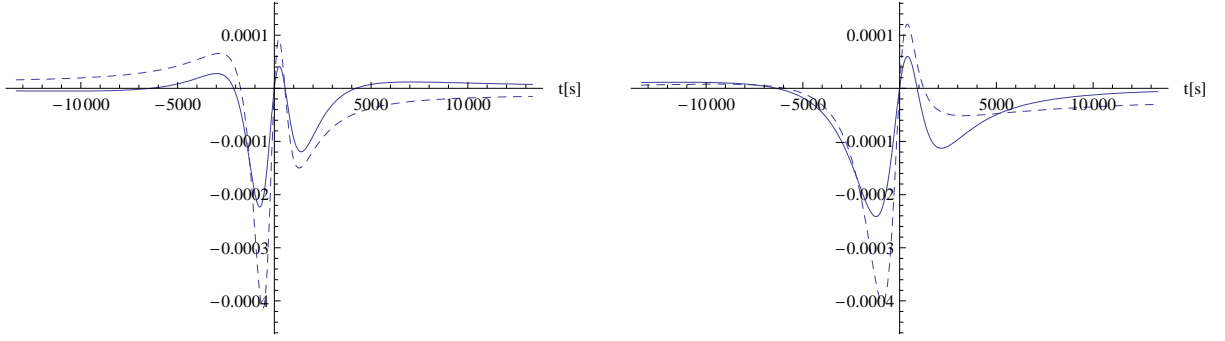


Figure 7: Time dependence of the first corrections to the waveform polarization states at 0.5PN order. Again, the corrections to the h_+ polarization are shown on the left and for h_\times on the right. The solid line shows the parabolic case and the dashed line shows $\epsilon = 2$ hyperbolic source. For further comparison amplitudes are multiplied by the factor 10^{20} .

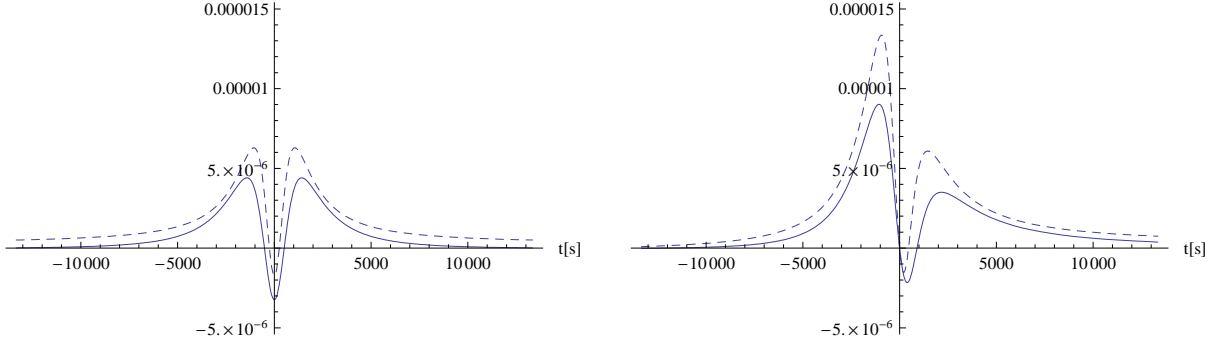


Figure 8: Multipolar corrections to the polarization states at 1PN order. Again, the corrections to h_+ are shown on the left and to h_\times on the right. Parabolic and hyperbolic orbit cases are depicted by solid and dashed lines, respectively. Again, the amplitudes are multiplied by the factor 10^{20} .

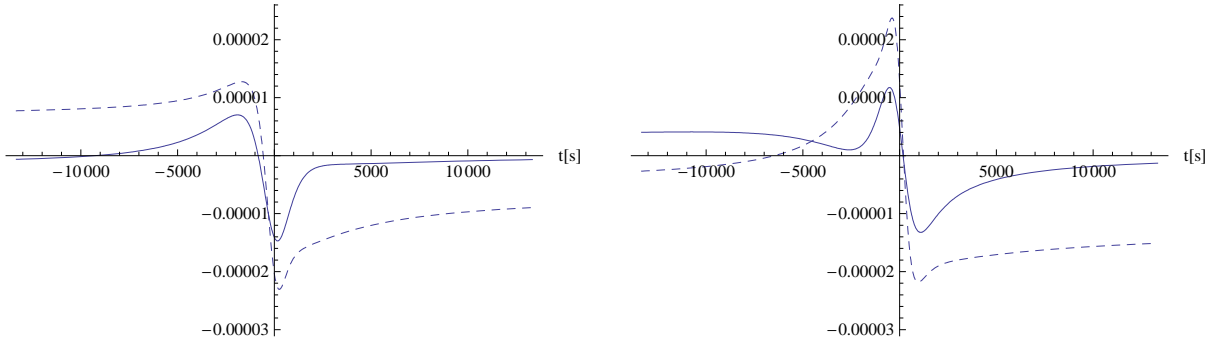


Figure 9: 1PN order corrections to the polarization states, which arise from the perturbative description of the elements of the motion. The notation is the same as on the former figures in this subsection. To compare the different terms of these corrections, the amplitudes are multiplied by the same factor as before, namely 10^{20} .

to a universal description valid for elliptic, parabolic and hyperbolic cases. The only differences are in the numerical integration determining the time dependence. With the use of this parametrization the radial and angular equations of the motion are solved, and with the inclusion of the results the analytic form of the polarization states for the emitted gravitational wave signals are evaluated for all types of sources including circular orbits, too.

The time dependence of the generalized true anomaly parameter χ is determined numerically for arbitrary parameter values. We have evaluated polarization states of the emitted radiation for realistic, and some well-known astrophysical sources. For elliptic orbits we presented the corrections to the waveform order by order for the Hulse-Taylor and J0737-3039 pulsars. For open orbits we have computed the waveforms for two sources with physically reasonable orbital elements to illustrate their main characteristics.

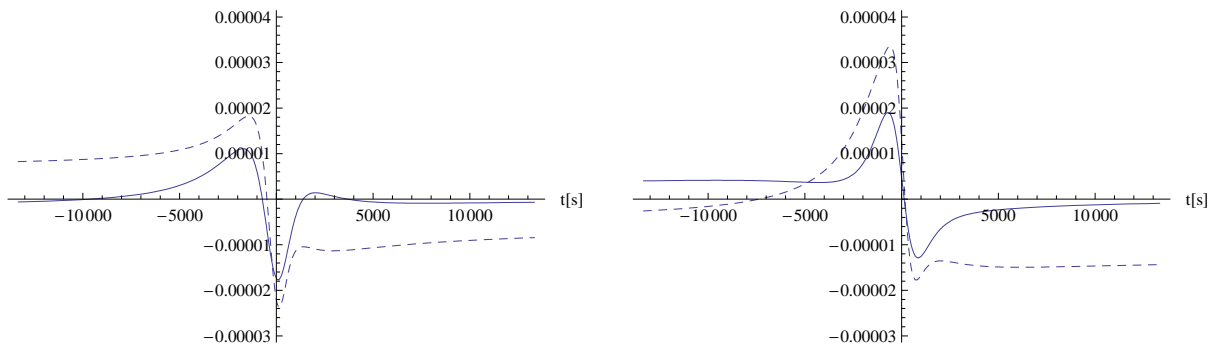


Figure 10: In these figures we plot the full 1PN corrections to the polarization states for the parabolic (solid line) and hyperbolic (dashed line) sources. The corrections to the h_+ polarization states are depicted on the left, while to h_\times on the right.

Our results illustrate the importance of the effects of eccentricity arising from the presence of higher harmonics in the waveform even at Newtonian order. The eccentricity increases the possibility of the detection of GWs emitted by sources on such orbits even if the eccentricity is very small, as it is in the case of the pulsar J0737-3039.

Our investigation of open orbit sources show that they provide unique, burstlike wave signals, and this behavior becomes more characteristic for higher order corrections. Meanwhile, these sources and the emitted waveforms can be described analytically, only the time dependence of the parameter has to be treated numerically. It gives the opportunity to investigate and create data banks for these sources to use matched filtering techniques.

Though the event rate estimations show that the detection of hyperbolic orbits are less probable, the emitted signal is more "spiky" for hyperbolic orbits than for parabolic ones with higher amplitude and frequency. These differences become more significant at higher PN order. We have chosen a quite large impact parameter (namely, almost equal to the periastron of the Hulse-Taylor pulsar) to compare the differences between closed and open orbit cases, and to investigate the effects of the eccentricity on the widest possible range. With the application of the parameter values chosen in [7], the frequency and the amplitude of the emitted waveform significantly increases.

The burstlike behavior of the waveform for open orbits, and the possibility of an analytic description, make these systems an important source of detectable gravitational waves for LISA. The significantly smaller impact parameter choice makes these systems potentially detectable for even the advanced ground-based detectors. The higher order description gives rise to many additional advantages, since it provides higher frequency terms for the matched filtering evaluations without the assumption of extreme parameter values for the astrophysical sources.

The results detailed above provide the possibility to generalize this formalism to describe spin and quadrupole effects on the detectable waveform. Furthermore, at higher orders it is possible to describe the closure of the orbit controlled by radiation reaction.

Acknowledgments

This work was supported by OTKA Grant No. NI68228. We would like to thank rpad Lukacs and Balazs Mikoczi for their valuable suggestions and help.

APPENDIX A: NEGLECTING INTERFERENCE TERMS IN $\chi(t)$

When solving Eq.(11) for elliptic orbits, the Newtonian and perturbative terms cannot be straightforwardly separated because of the secular divergences. The easiest way to solve the differential equation numerically is to solve the Newtonian and 1PN order equations with either the integration of the differential equations or with the inversion of the analytic solution $t(\chi)$.

When the different order contributions in the resulting numerical data are to be separated it is nontrivial to neglect the interference terms. In the following we give the description of the problem, and give the guidelines for the solution.

The Newtonian order equation has the following structure

$$\frac{d\chi_N}{dt} = f_N(\cos \chi_N), \quad (26)$$

and similarly the 1PN order equation is

$$\frac{d\chi}{dt} = f(\cos \chi) , \quad (27)$$

where

$$f(\cos \chi) = f_N(\cos \chi) + f_P(\cos \chi) ,$$

and we wish to find the solution of the form

$$\chi_N = \Omega_N t + g_N(t) , \quad \chi = (\Omega_N + \Omega_P)t + g(t) . \quad (28)$$

Using the above results one can evaluate both the $g_N(t)$ and $g(t)$ functions (Ω_N and Ω_P are known from analytic evaluations, see Sec. III.B.). To be able to determine the contributions of the different order to the

$$\chi = (\Omega_N + \Omega_P)t + \tilde{g}_N(t) + g_P(t) \quad (29)$$

solution, our main goal is to determine the function $\tilde{g}_N(t)$.

To achieve this we rewrite the above differential equations as

$$\frac{dg_N(t)}{dt} = f_N(\cos [\Omega_N t + g_N(t)]) - \Omega_N \quad (30)$$

and

$$\begin{aligned} \frac{d[\tilde{g}_N(t) + g_P(t)]}{dt} &= f_N(\cos [(\Omega_N + \Omega_P)t + \tilde{g}_N(t)] - g_P(t) \sin [(\Omega_N + \Omega_P)t + \tilde{g}_N(t)]) \\ &+ f_P(\cos [(\Omega_N + \Omega_P)t + \tilde{g}_N(t)] - (\Omega_N + \Omega_P) + o(\epsilon^2) . \end{aligned}$$

After introducing the

$$t' = \frac{\Omega_N - \Omega_P}{\Omega_N} t$$

variable we will analyze the equation

$$\begin{aligned} \frac{d[\tilde{g}_N(t') + g_P(t')]}{dt} &= f_N(\cos [\Omega_N t + \tilde{g}_N(t')] - g_P(t') \sin [\Omega_N t + \tilde{g}_N(t')]) \left(1 - \frac{\Omega_P}{\Omega_N}\right) \\ &+ f_P(\cos [\Omega_N t + \tilde{g}_N(t')] - \Omega_N + o(\epsilon^2) . \end{aligned}$$

This equation will become

$$\left. \frac{d\tilde{g}_N(t')}{dt} \right|_N = f_N(\cos [\Omega_N t + \tilde{g}_N(t')] - \Omega_N \quad (31)$$

at the Newtonian order. Comparing it with Eq.(30) it turns out that

$$\tilde{g}(t') = g_N(t) = g_N \left(\left[1 + \frac{\Omega_P}{\Omega_N} \right] t' \right) .$$

With the use of it the whole solution of the problem is

$$\chi = (\Omega_N + \Omega_P)t + g_N \left(\left[1 + \frac{\Omega_P}{\Omega_N} \right] t \right) + \left(g(t) - g_N \left(\left[1 + \frac{\Omega_P}{\Omega_N} \right] t \right) \right) , \quad (32)$$

where $g_N(t)$ and $g(t)$ are to be determined numerically, Ω_N and Ω_P are evaluated analytically.

APPENDIX B: CONSTANT COEFFICIENTS FOR THE WAVEFORM EXPRESSIONS

Our analytic calculations give rise to complicated expressions for the polarization states of the gravitational wave signals in all relevant cases. In the previous sections the main structure of the waveforms was given and their main properties were analyzed. In this Appendix we collect the explicit form of the constant coefficients appearing in the waveform expressions.

We start by introducing the following short-hand notations:

$$\begin{aligned}
K &= 1 - 3\eta, & B &= 8 - 3\eta, & D &= \frac{m\mu}{A_0}, \\
A_1^N &= \frac{A_0^2}{4L^2}, & A_2^N &= \frac{A_0 m \mu}{8L^2}, & A_3^N &= \frac{m^2 \mu^2}{2L^2}, \\
A_4^N &= \frac{A_0^3 m \mu}{8L^4}, & A_5^N &= \frac{A_0^2 m^2 \mu^2}{16L^4}, & A_6^N &= \frac{A_0 m^3 \mu^3}{4L^4}, & A_7^N &= \frac{E^2}{16\mu^2}, & A_8^N &= \frac{m^2 \mu E}{8L^2}, & A_9^N &= \frac{m^4 \mu^4}{16L^4}, \\
A_{10}^N &= DA_7^N, & A_{11}^N &= DA_8^N, & A_{12}^N &= DA_9^N, \\
A_1^{0.5} &= \frac{\delta m A_0^3}{256L^3 m}, & A_2^{0.5} &= \frac{\delta m A_0^2 \mu}{128L^3}, & A_3^{0.5} &= \frac{\delta m A_0 m \mu^2}{64L^3}, & A_4^{0.5} &= \frac{\delta m m^2 \mu^3}{32L^3}, \\
A_1^1 &= \frac{A_0^4}{64L^4}, & A_2^1 &= A_4^N / 384, & A_3^1 &= A_5^N / 48, & A_4^1 &= A_6^N / 384, & A_5^1 &= A_9^N / 3.
\end{aligned} \tag{33}$$

Although the above coefficients are not independent, they are introduced separately to keep our tables clear and well-defined.

As it can be seen from the results of Sec. VI. in the analytic waveform expressions, Eqs.(23), the coefficients C_F and S_F of χ and χ' are time independent. These coefficients depend on the different harmonics of the angle γ and we introduce the following general decomposition valid at least up to 1PN order and for both polarization states:

$$\begin{aligned}
C_F &= \sum_{l=0}^{\infty} \left[a_l^{C_F} \sin(l\gamma) + b_l^{C_F} \cos(l\gamma) \right], \\
S_F &= \sum_{l=0}^{\infty} \left[a_l^{S_F} \sin(l\gamma) + b_l^{S_F} \cos(l\gamma) \right].
\end{aligned} \tag{34}$$

Here F is a multi-index containing the index of the polarization state, the PN order of the expression, and the index of the harmonics of χ and/or χ' . The coefficients $a_l^{C_F}$, $b_l^{C_F}$, $a_l^{S_F}$, and $b_l^{S_F}$ in Eq.(34) will be given in tabular form for both polarization states and PN orders. Any coefficients $a_l^{C_F}$, $b_l^{C_F}$, $a_l^{S_F}$ and $b_l^{S_F}$ not listed in the tables are identically zero. With the use of these coefficients listed in the tables the quantities C_F and S_F in Eq.(34) are easily reconstructed.

A. Circular orbit case

Let us recall the results presented in Sec. VI.B. The polarization states for the detectable gravitational wave signal can be written as

$$h^{N\ddot{x}} = \sum_{k=0}^2 [C_k^{N\ddot{x}} \cos(k\chi') + S_k^{N\ddot{x}} \sin(k\chi')], \tag{35}$$

$$h^{0.5\ddot{x}} = \sum_{k=0}^3 [C_k^{0.5\ddot{x}} \cos(k\chi') + S_k^{0.5\ddot{x}} \sin(k\chi')], \tag{36}$$

$$h^{1\ddot{x}} = \sum_{k=0}^4 [C_k^{1\ddot{x}} \cos(k\chi') + S_k^{1\ddot{x}} \sin(k\chi')], \tag{37}$$

where

$$\chi' = \Upsilon_0 + \frac{Lt}{\mu r^2} - \frac{Lt}{\mu^2 r^3} [(1 - 3\eta)Er + (4 - 2\eta)m\mu].$$

Instead of using the short-hand notations of Eq.(33), we use the following expressions:

$$\begin{aligned} a_1^N &= \frac{L^2}{4r^2\mu^2}, & a_2^N &= \frac{m}{4r}, & a_3^N &= (1-3\eta)\frac{EL^2}{2r^2\mu^3}, & a_4^N &= (2-\eta)\frac{L^2m}{r^3\mu^2}, \\ a_1^{0.5} &= \frac{\delta mL^3}{32m\mu^3r^3}, & a_2^{0.5} &= \frac{\delta mL}{32\mu r^2}, \\ a_1^1 &= \frac{L^4}{384\mu^4r^4}, & a_2^1 &= \frac{L^2m}{384\mu^2r^3}, & a_3^1 &= \frac{m^2}{384r^2}. \end{aligned}$$

As an example, the Newtonian expression for C_2^{N+} arising with the use of Table III as

$$C_2^{N+} = b_2^{C_2^{N+}} \cos 2\gamma + b_0^{C_2^{N+}} = (a_1^N + a_2^N) \cos 2\gamma + 3(a_1^N + a_2^N). \quad (38)$$

The relevant coefficients for circular orbits are listed in Tables III - VII.

State	+		×
Harmonic	$\cos 2\gamma$	1	$\cos \gamma$
C_2^N	$a_1^N + a_2^N$	$3(a_1^N + a_2^N)$	0
C_0^N	$-a_1^N + a_2^N$	$a_1^N - a_2^N$	0
S_2^N	0	0	$4(a_1^N + a_2^N)$

Table III: This table contains the relevant $b_l^{C_k}$ and $b_l^{S_k}$ coefficients for evaluating every C_k^N and S_k^N in Eq.(35) restricted to the Newtonian order. Any other coefficients are zero. The column under the sign "+" contains the coefficients for h^{N+} , and under the sign "×" the coefficients for $h^{N\times}$ can be found.

State	+		×
Harmonic	$\sin 3\gamma$	$\sin \gamma$	$\sin 2\gamma$
$C_3^{0.5}$	$-4a_1^{0.5}$	$-20a_1^{0.5}$	$8a_1^{0.5} - 28a_2^{0.5}$
$C_1^{0.5}$	$4a_1^{0.5}$	$20a_1^{0.5}$	$-8a_1^{0.5} - 20a_2^{0.5}$
$S_3^{0.5}$	$-2a_1^{0.5} + 7a_2^{0.5}$	$5(-2a_1^{0.5} + 7a_2^{0.5})$	$-16a_1^{0.5}$
$S_1^{0.5}$	$6a_1^{0.5} + 7a_2^{0.5}$	$-2a_1^{0.5} + 19a_2^{0.5}$	$16a_1^{0.5}$

Table IV: This table details the relevant coefficients for evaluating every C_k^N and S_k^N in Eq.(36) for both polarization states. The coefficients not included are zero. Again, the column under the sign "+" contains the coefficients for $h^{0.5+}$, and under the sign "×" the coefficients for $h^{0.5\times}$ can be found.

Harmonic	$\cos 4\gamma$	$\cos 2\gamma$	1
C_4^1	$K(6a_1^1 + 51a_2^1 + 7a_3^1)$	$4K(6a_1^1 + 51a_2^1 + 7a_3^1)$	$5K(6a_1^1 + 51a_2^1 + 7a_3^1)$
C_2^1	$4K(-6a_1^1 + 3a_2^1 + 7a_3^1)$	$16[3Ka_1^1 + 9(1+K)a_2^1 - 29a_3^1]$	$4[42Ka_1^1 + 3(7+87\eta)a_2^1 + (-355+21\eta)a_3^1]$
C_0^1	$3K(6a_1^1 - 13a_2^1 + 7a_3^1)$	$12[-6Ka_1^1 + (23-17\eta)a_2^1 + (-41+7\eta)a_3^1]$	$3[18Ka_1^1 + (-79+29\eta)a_2^1 + (157-7\eta)a_3^1]$

Table V: This table details the relevant coefficients for evaluating every nonzero C_k^1 in Eq.(37) for h^{1+} . It is worth mentioning that in this case all S_k^1 are zero.

B. Elliptic orbit case

Here we recall the results discussed in Sec. VI. A to collect all the expressions for the elliptic orbit case:

$$h^{N\times} = \sum_{k=-2}^2 \sum_{j=-3}^3 [C_{k,j}^{N\times} \cos(k\chi' + j\chi) + S_{k,j}^{N\times} \sin(k\chi' + j\chi)], \quad (39)$$

Harmonic	$\cos 3\gamma$	$\cos \gamma$
S_4^1	$4K(6a_1^1 + 51a_2^1 + 7a_3^1)$	$4K(6a_1^1 + 51a_2^1 + 7a_3^1)$
S_2^1	$8K(-6a_1^1 + 15a_2^1 + 7a_3^1)$	$8[30Ka_1^1 + 3(11 + 39\eta)a_2^1 + (-239 + 21\eta)a_3^1]$

Table VI: This table details the relevant coefficients for evaluating every nonzero S_k^1 in Eq.(37) for $h^{1\times}$. It is worth mentioning that in this case all C_k^1 are zero.

State	+		\times
Harmonic	$\cos 2\gamma$	1	$\cos \gamma$
C_2^N	$a_1^N + a_2^N - (a_3^N + a_4^N)$	$3(a_1^N + a_2^N) - 3(a_3^N + a_4^N)$	0
C_0^N	$-a_1^N + a_2^N + (a_3^N + a_4^N)$	$a_1^N - a_2^N - (a_3^N + a_4^N)$	0
S_2^N	0	0	$4(a_1^N + a_2^N) - 4(a_3^N + a_4^N)$

Table VII: In this table the full coefficients are presented for Eq.(35), including 1PN order terms from the corrections of the description of the motion. The table is organized in the same way as Table III.

$$h^{0.5\times} = \sum_{k,j=-3}^3 [C_{k,j}^{0.5\times} \cos(k\chi' + j\chi) + S_{k,j}^{0.5\times} \sin(k\chi' + j\chi)] , \quad (40)$$

$$h^{1\times} = \sum_{k,j=-4}^4 [C_{k,j}^{1\times} \cos(k\chi' + j\chi) + S_{k,j}^{1\times} \sin(k\chi' + j\chi)] , \quad (41)$$

where

$$\chi' = \Upsilon_0 + \chi - \frac{3m^2\mu^2}{L^2}\chi .$$

Again, to collect the explicit expressions for the $C_{k,j}$ and $S_{k,j}$ constant quantities we will use the short-hand notations and definitions of Eq.(33) and Eq.(34).

For elliptic orbits our tables are organized in the same way as in the circular orbit case. As an example, we detail the expression of $C_{4,1}^{1+}$ with the use of Table X:

$$\begin{aligned} C_{4,1}^{1+} &= b_4^{C_{4,1}^{1+}} \cos[4\gamma] + b_2^{C_{4,1}^{1+}} \cos[2\gamma] + b_0^{C_{4,1}^{1+}} \\ &= (K81A_2^1 + K452A_4^1) \cos[4\gamma] + (324KA_2^1 + 1808KA_4^1) \cos[2\gamma] - (405KA_2^1 + 2260KA_4^1) . \end{aligned} \quad (42)$$

The relevant coefficients for elliptic orbits are listed in Tables VIII - XIII.

State	+		State	\times
Harmonic	$\cos 2\gamma$	1	Harmonic	$\cos \gamma$
$C_{2,1}^N$	A_2^N	$3A_2^N$	$S_{2,1}^N$	$4A_2^N$
$C_{2,0}^N$	A_3^N	$3A_3^N$	$S_{2,0}^N$	$4A_3^N$
$C_{2,-1}^N$	$5A_2^N$	$15A_2^N$	$S_{-2,2}^N$	$-4A_1^N$
$C_{2,-2}^N$	A_1^N	$3A_1^N$	$S_{-2,1}^N$	$-20A_2^N$
$C_{0,1}^N$	$-A_2^N$	A_2^N		
$C_{0,0}^N$	$-A_1^N$	A_1^N		

Table VIII: This table contains the relevant $b_i^{C_{k,j}}$ and $b_i^{S_{k,j}}$ coefficients for evaluating every non-zero $C_{k,j}^N$ and $S_{k,j}^N$ in Eq.(39) restricted to the Newtonian order. The left table contains the coefficients for h^{N+} , and in the right one the coefficients for $h^{N\times}$ can be found. It is worth to mention that for the "plus" state every S_k^N , and for the "cross" state every C_k^N are zero.

Tables XII and XIII contain the 1PN corrections to the Newtonian coefficients given in Table VIII, from which the full coefficients in Eq.(39) can be reconstructed.

State	+		×
harmonic	$\sin 3\gamma$	$\sin \gamma$	$\sin 2\gamma$
$C_{3,3}^{0.5}$	$-4A_1^{0.5}$	$-20A_1^{0.5}$	$-4A_1^{0.5}$
$C_{3,2}^{0.5}$	$-12A_2^{0.5}$	$-60A_2^{0.5}$	$-4A_2^{0.5}$
$C_{3,1}^{0.5}$	$-4(3A_1^{0.5} + A_3^{0.5})$	$-4(15A_1^{0.5} + A_3^{0.5})$	$4(11A_1^{0.5} - 2A_3^{0.5})$
$C_{3,0}^{0.5}$	$-4(6A_2^{0.5} + A_4^{0.5})$	$-20(6A_2^{0.5} + A_4^{0.5})$	$20(2A_2^{0.5} - A_4^{0.5})$
$C_{3,-1}^{0.5}$	$-12(A_1^{0.5} + A_3^{0.5})$	$-60(A_1^{0.5} + A_3^{0.5})$	$4(13A_1^{0.5} - 14A_3^{0.5})$
$C_{3,-2}^{0.5}$	$-12A_2^{0.5}$	$-60A_2^{0.5}$	$-60A_2^{0.5}$
$C_{3,-3}^{0.5}$	$-4A_1^{0.5}$	$-20A_1^{0.5}$	$-28A_1^{0.5}$
$C_{1,3}^{0.5}$	$4A_1^{0.5}$	$4A_1^{0.5}$	$-4A_1^{0.5}$
$C_{1,2}^{0.5}$	$12A_2^{0.5}$	$60A_2^{0.5}$	$-20A_2^{0.5}$
$C_{1,1}^{0.5}$	$12(A_1^{0.5} + A_3^{0.5})$	$60(A_1^{0.5} + A_3^{0.5})$	$-20(A_1^{0.5} + 2A_3^{0.5})$
$C_{1,0}^{0.5}$	$4(6A_2^{0.5} + A_4^{0.5})$	$20(6A_2^{0.5} + A_4^{0.5})$	$-4(18A_2^{0.5} + 7A_4^{0.5})$
$C_{1,-1}^{0.5}$	$12(A_1^{0.5} + A_3^{0.5})$	$60(A_1^{0.5} + A_3^{0.5})$	$-4(3A_1^{0.5} + 22A_3^{0.5})$
$C_{1,-2}^{0.5}$	$12A_2^{0.5}$	$60A_2^{0.5}$	$-84A_2^{0.5}$
$C_{1,-3}^{0.5}$	$4A_1^{0.5}$	$20A_1^{0.5}$	$-28A_1^{0.5}$
$S_{3,3}^{0.5}$	$A_1^{0.5}$	$5A_1^{0.5}$	$-16A_1^{0.5}$
$S_{3,2}^{0.5}$	$-A_2^{0.5}$	$-5A_2^{0.5}$	$-48A_2^{0.5}$
$S_{3,1}^{0.5}$	$-11A_1^{0.5} + 2A_3^{0.5}$	$-5(11A_1^{0.5} - 2A_3^{0.5})$	$-48(A_1^{0.5} + A_3^{0.5})$
$S_{3,0}^{0.5}$	$-5(2A_2^{0.5} - A_4^{0.5})$	$-25(2A_2^{0.5} - A_4^{0.5})$	$-16(6A_2^{0.5} + A_4^{0.5})$
$S_{1,3}^{0.5}$	$11A_1^{0.5}$	$-25A_1^{0.5}$	$16A_1^{0.5}$
$S_{1,2}^{0.5}$	$23A_2^{0.5}$	$-29A_2^{0.5}$	$48A_2^{0.5}$
$S_{1,1}^{0.5}$	$-23A_1^{0.5} - 22A_3^{0.5}$	$-29A_1^{0.5} + 14A_3^{0.5}$	$48(A_1^{0.5} + A_3^{0.5})$
$S_{1,0}^{0.5}$	$38A_2^{0.5} + 13A_4^{0.5}$	$-30A_2^{0.5} - 17A_4^{0.5}$	$16(6A_2^{0.5} + A_4^{0.5})$
$S_{-1,3}^{0.5}$	$-13A_1^{0.5}$	$-17A_1^{0.5}$	$-16A_1^{0.5}$
$S_{-1,2}^{0.5}$	$-39A_2^{0.5}$	$-51A_2^{0.5}$	$-48A_2^{0.5}$
$S_{-1,1}^{0.5}$	$-A_1^{0.5} - 93/2A_3^{0.5}$	$-21A_1^{0.5} - 50A_3^{0.5}$	$-16(A_1^{0.5} + A_3^{0.5})$
$S_{-3,3}^{0.5}$	$-7A_1^{0.5}$	$-35A_1^{0.5}$	$16A_1^{0.5}$
$S_{-3,2}^{0.5}$	$-15A_2^{0.5}$	$-75A_2^{0.5}$	$48A_2^{0.5}$
$S_{-3,1}^{0.5}$	$13A_1^{0.5} - 14A_3^{0.5}$	$5(13A_1^{0.5} - 14A_3^{0.5})$	$48(A_1^{0.5} + A_3^{0.5})$

Table IX: This table contains the relevant $a_l^{C_{k,j}}$ and $a_l^{S_{k,j}}$ coefficients for evaluating the explicit form of Eq.(40). Any other coefficients are zero in this equation. The columns under the sign "+" contains the coefficients for $h^{0.5+}$ and under the sign "×" the coefficients for $h^{0.5×}$ can be found.

C. Open orbit case

For open orbits the structure of the polarization states of the gravitational waves can be written as

$$h^{N+} = \chi \sum_{k=0}^3 [C_{k\chi}^{N+} \cos(k\chi) + S_{k\chi}^{N+} \sin(k\chi)] + \sum_{k=0}^4 [C_k^{N+} \cos(k\chi) + S_k^{N+} \sin(k\chi)] , \quad (43)$$

$$h^{0.5+} = \sum_{k=0}^6 [C_k^{0.5+} \cos(k\chi) + S_k^{0.5+} \sin(k\chi)] , \quad (44)$$

$$h^{1+} = \sum_{k=0}^7 [C_k^{1+} \cos(k\chi) + S_k^{1+} \sin(k\chi)] . \quad (45)$$

In this case there are no secular terms in the approximation scheme, and hence a more straightforward series expansion can be given. It makes the structure of the waveform expressions simpler, but on the other hand the

Harmonic	$\cos [4\gamma]$	$\cos [2\gamma]$	1
$C_{4,3}^{1+}$	$15KA_2^1$	$60KA_2^1$	$-75KA_2^1$
$C_{4,2}^{1+}$	$35KA_3^1$	$140KA_3^1$	$-175KA_3^1$
$C_{4,1}^{1+}$	$K81A_2^1 + K452A_4^1$	$324KA_2^1 + 1808KA_4^1$	$-405KA_2^1 - 2260KA_4^1$
$C_{4,0}^{1+}$	$142KA_3^1 + 16KA_5^1$	$568KA_3^1 + 32KA_5^1$	$-710KA_3^1 - 40KA_5^1$
$C_{4,-1}^{1+}$	$189KA_2^1 + 1076KA_4^1$	$756KA_2^1 + 4304KA_4^1$	$-945KA_2^1 - 5380KA_4^1$
$C_{4,-2}^{1+}$	$215KA_3^1$	$860KA_3^1$	$-1075KA_3^1$
$C_{4,-3}^{1+}$	$315KA_2^1$	$1260KA_2^1$	$-1575KA_2^1$
$C_{4,-4}^{1+}$	KA_1^1	$4KA_1^1$	$-5KA_1^1$
$C_{2,3}^{1+}$	$-24KA_2^1$	$96(2 - 9\eta)A_2^1$	$24(1 - 39\eta)A_2^1$
$C_{2,2}^{1+}$	$-40KA_3^1$	$8(4 - 123\eta)A_3^1$	$-8(103 + 243\eta)A_3^1$
$C_{2,1}^{1+}$	$-144KA_2^1 - 256KA_4^1$	$96(5 - 14\eta)A_2^1 - 64(13 + 144\eta)A_4^1$	$48(39\eta - 11)A_2^1 + 64(42\eta - 167)A_4^1$
$C_{2,0}^{1+}$	$-152KA_3^1 + 2KA_5^1$	$16(34 - 123\eta)A_3^1 - 8(2 + 9\eta)A_5^1$	$8(69\eta - 65)A_3^1 + 2(39\eta - 73)A_5^1$
$C_{2,-1}^{1+}$	$-504KA_2^1 + 224KA_4^1$	$96(45\eta - 22)A_2^1 - 64(29 - 120\eta)A_4^1$	$8(543 - 873\eta)A_2^1 + 32(237\eta - 145)A_4^1$
$C_{2,-2}^{1+}$	$-4KA_1^1 + 32KA_3^1$	$8KA_1^1 + 8(100 - 171\eta)A_3^1$	$28KA_1^1 + 336(128 + 3\eta)A_3^1$
$C_{2,-3}^{1+}$	0	$96(11 - 16\eta)A_2^1$	$96(23 - 18\eta)A_2^1$
$C_{0,3}^{1+}$	$30KA_2^1$	$24(29 - 15\eta)A_2^1$	$6(75\eta - 121)A_2^1$
$C_{0,2}^{1+}$	$-30KA_3^1$	$120(1 + 3\eta)A_3^1$	$-30(5 + 9\eta)A_3^1$
$C_{0,1}^{1+}$	$234KA_2^1 - 24KA_4^1$	$24(235\eta - 33)A_2^1 - 96(37 - 35\eta)A_4^1$	$6(93 - 823\eta)A_2^1 + 24(149 - 143\eta)A_4^1$
$C_{0,0}^{1+}$	$3KA_1^1 - 6KA_3^1$	$-12KA_1^1 + 24(13 - 49\eta)A_3^1 + 12(3 - \eta)A_5^1$	$9KA_1^1 + 6(53 - 199\eta)A_3^1 + 12(3 - \eta)A_5^1$

Table X: This table details the relevant coefficients for evaluating every nonzero $C_{k,j}$ in Eq.(41) for h^{1+} . It is worth mentioning that for h^{1+} every $S_{k,j}$ are zero.

Harmonic	$\cos [3\gamma]$	$\cos [\gamma]$
$S_{4,3}^{1\times}$	$60KA_2^1$	$-60KA_2^1$
$S_{4,2}^{1\times}$	$140KA_3^1$	$-140KA_3^1$
$S_{4,1}^{1\times}$	$324KA_2^1 + 1808KA_4^1$	$-324KA_2^1 + 1808KA_4^1$
$S_{4,0}^{1\times}$	$568KA_3^1 + 32KA_5^1$	$-568KA_3^1 + 32KA_5^1$
$S_{2,3}^{1\times}$	$24KA_2^1$	$24(7 - 69\eta)A_2^1$
$S_{2,2}^{1\times}$	$40KA_3^1$	$-8(109 + 117\eta)A_3^1$
$S_{2,1}^{1\times}$	$-24KA_2^1 + 544KA_4^1$	$24(37\eta - 7)A_2^1 - 32(585 + 69\eta)A_4^1$
$S_{2,0}^{1\times}$	$16KA_3^1 - 16KA_5^1$	$-112(1 + 9\eta)A_3^1 - 16(11 - 3\eta)A_5^1$
$S_{0,3}^{1\times}$	$-48KA_2^1$	$48KA_2^1$
$S_{0,2}^{1\times}$	$-48KA_3^1$	$48KA_3^1$
$S_{0,1}^{1\times}$	$-48KA_2^1 + 192KA_4^1$	$48KA_2^1 + 192KA_4^1$
$S_{-2,3}^{1\times}$	$-120KA_2^1$	$24(121\eta - 131)A_2^1$
$S_{-2,2}^{1\times}$	$8KA_1^1 - 232KA_3^1$	$-40KA_1^1 - 8(203 - 93\eta)A_3^1$
$S_{-2,1}^{1\times}$	$672KA_2^1 - 1696KA_4^1$	$24(495\eta - 277)A_2^1 + 32(133 - 135\eta)A_4^1$
$S_{-4,4}^{1\times}$	$-4KA_1^1$	$4KA_1^1$
$S_{-4,3}^{1\times}$	$-1260KA_2^1$	$1260KA_2^1$
$S_{-4,2}^{1\times}$	$-860KA_3^1$	$860KA_3^1$
$S_{-4,1}^{1\times}$	$-756KA_2^1 - 4304KA_4^1$	$756KA_2^1 + 4304KA_4^1$

Table XI: This table details the relevant coefficients for evaluating every nonzero $S_{k,j}$ in Eq.(41) for $h^{1\times}$. It is worth mentioning that for $h^{1\times}$ every $C_{k,j}$ are zero.

expressions for each coefficient become significantly more complex. It is because in addition to the harmonics of the

Harmonic	$\cos [2\gamma]$	1
$C_{2,2}^{N+}$	$-BA_5^N$	$-3BA_5^N$
$C_{2,1}^{N+}$	$(13\eta - 31)A_{10}^N - (10 - 9\eta)A_{11}^N - 2(14 - 17\eta)A_{12}^N$	$3(13\eta - 31)A_{10}^N - 3(10 - 9\eta)A_{11}^N - 6(14 - 17\eta)A_{12}^N$
$C_{2,0}^{N+}$	$2(5\eta - 3)A_8^N + 8(5\eta - 2)A_9^N$	$6(5\eta - 3)A_8^N + 24(5\eta - 2)A_9^N$
$C_{2,-1}^{N+}$	$(65\eta - 51)A_{10}^N - (32 - 43\eta)A_{11}^N - 2(18 - 23\eta)A_{12}^N$	$3(65\eta - 51)A_{10}^N - 3(32 - 43\eta)A_{11}^N - 6(18 - 23\eta)A_{12}^N$
$C_{2,-2}^{N+}$	$-12KA_7^N + (33\eta - 32)A_8^N + (53\eta - 48)A_9^N$	$-36KA_7^N + 3(33\eta - 32)A_8^N + 3(53\eta - 48)A_9^N$
$C_{2,-3}^{N+}$	$(3\eta - 4)A_4^N$	$3(3\eta - 4)A_4^N$
$C_{0,3}^{N+}$	$2(2 - \eta)A_4^N$	$6(\eta - 2)A_4^N$
$C_{0,2}^{N+}$	$(5 - 4\eta)A_8^N + 4(12 - 11\eta)A_9^N$	$4(4\eta - 5)A_8^N - 4(12 - 11\eta)A_9^N$
$C_{0,1}^{N+}$	$2(43 - 49\eta)A_{10}^N + 2(41 - 34\eta)A_{11}^N + 4(28 - 25\eta)A_{12}^N$	$2(49\eta - 43)A_{10}^N - 2(41 - 34\eta)A_{11}^N - 4(28 - 25\eta)A_{12}^N$
$C_{0,0}^{N+}$	$12KA_7^N + 2(21 - 19\eta)A_8^N + 12(6 - 5\eta)A_9^N$	$-12KA_7^N - 2(21 - 19\eta)A_8^N - 12(6 - 5\eta)A_9^N$
$S_{2,0}^{N+}$	$-4BA_5^N$	$-12BA_5^N$
$S_{0,1}^{N+}$	$2BA_4^N$	$-2BA_4^N$
$S_{-2,1}^{N+}$	$2BA_4^N$	$6BA_4^N$

Table XII: 1PN corrections to the coefficients for h^{N+} in Eq.(39). The table contains all coefficients to evaluate each nonzero $C_{k,j}$ and $S_{k,j}$. Any other coefficients for these expressions are zero.

Harmonic	$\cos [\gamma]$
$C_{2,0}^{N\times}$	$16BA_5^N$
$C_{2,-1}^{N\times}$	$8BA_4^N$
$S_{2,2}^{N\times}$	$-4BA_5^N$
$S_{2,1}^{N\times}$	$4(13\eta - 31)A_{10}^N - 4(10 - 9\eta)A_{11}^N - 8(14 - 17\eta)A_{12}^N$
$S_{2,0}^{N\times}$	$8(5\eta - 3)A_8^N - 32(2 - 5\eta)A_9^N$
$S_{-2,3}^{N\times}$	$4(4 - 3\eta)A_4^N$
$S_{-2,2}^{N\times}$	$48KA_7^N + 4(32 - 33\eta)A_8^N + 4(48 - 53\eta)A_9^N$
$S_{-2,1}^{N\times}$	$4(51 - 65\eta)A_{10}^N + 4(32 - 43\eta)A_{11}^N + 8(18 - 23\eta)A_{12}^N$

Table XIII: 1PN corrections to the coefficients for $h^{N\times}$ in Eq.(39). The table contains all coefficients to evaluate each nonzero $S_{k,j}$ and $C_{k,j}$. Any other coefficients for these expressions are zero.

angle γ there appear the harmonics of Υ_0 , too.

To keep our tables simple we introduce the following short-hand notations:

$$\begin{aligned}
C_k^{N+} &= C_{kC2}^{N+} \cos [2\gamma] + C_{k0}^{N+}, & S_k^{N+} &= S_{kC2}^{N+} \cos [2\gamma] + S_{k0}^{N+} \\
C_k^{N\times} &= C_{kC1}^{N\times} \cos [\gamma], & S_k^{N\times} &= S_{kC1}^{N\times} \cos [\gamma] \\
C_k^{0.5+} &= C_{kS3}^{0.5+} \sin [3\gamma] + C_{kS1}^{0.5+} \sin [\gamma], & S_k^{0.5+} &= S_{kS3}^{0.5+} \sin [3\gamma] + S_{kS1}^{0.5+} \sin [\gamma] \\
C_k^{0.5\times} &= C_{kS2}^{0.5\times} \sin [2\gamma], & S_k^{0.5\times} &= S_{kS2}^{0.5\times} \sin [2\gamma] \\
C_k^{1+} &= C_{kC4}^{1+} \cos [4\gamma] + C_{kC2}^{1+} \cos [2\gamma] + C_{k0}^{1+}, & S_k^{1+} &= S_{kC4}^{1+} \cos [4\gamma] + S_{kC2}^{1+} \cos [2\gamma] + S_{k0}^{1+} \\
C_k^{1\times} &= C_{kC3}^{1\times} \cos [3\gamma] + C_{kC1}^{1\times} \cos [\gamma], & S_k^{1\times} &= S_{kC3}^{1\times} \cos [3\gamma] + S_{kC1}^{1\times} \cos [\gamma].
\end{aligned} \tag{46}$$

For open orbits we separate the higher harmonics in Υ_0 instead of γ , and hence we write

$$\begin{aligned}
C_F &= \sum_{l=0}^{\infty} \left[a_l^{C_F} \sin (l\Upsilon_0) + b_l^{C_F} \cos (l\Upsilon_0) \right], \\
S_F &= \sum_{l=0}^{\infty} \left[a_l^{S_F} \sin (l\Upsilon_0) + b_l^{S_F} \cos (l\Upsilon_0) \right],
\end{aligned} \tag{47}$$

where F is also a multi-index as for the elliptic case containing also the index of the harmonics of γ . Tables XIV-XXIV contain all the relevant $a_l^{C_F}$, $b_l^{C_F}$, $a_l^{S_F}$ and $b_l^{S_F}$ coefficients. Any other a_l or b_l coefficients are zero.

Harmonic	$\cos 2\Upsilon_0$	$\sin 2\Upsilon_0$	1
C_{3C2}^N	A_2^N	0	0
C_{2C2}^N	A_3^N	0	0
C_{1C2}^N	$5A_2^N$	0	$-2A_2^N$
C_{0C2}^N	A_1^N	0	$-A_1^N$
C_{30}^N	$3A_2^N$	0	0
C_{20}^N	$3A_3^N$	0	0
C_{10}^N	$15A_2^N$	0	$2A_2^N$
C_{00}^N	$3A_1^N$	0	A_1^N
S_{3C2}^N	0	$-A_2^N$	0
S_{2C2}^N	0	$-A_3^N$	0
S_{1C2}^N	0	$-5A_2^N$	0
S_{30}^N	0	$-3A_2^N$	0
S_{20}^N	0	$-3A_3^N$	0
S_{10}^N	0	$-15A_2^N$	0

Harmonic	$\cos 2\Upsilon_0$	$\sin 2\Upsilon_0$
C_{3C1}^N	0	$4A_2^N$
C_{2C1}^N	0	$4A_3^N$
C_{1C1}^N	0	$20A_2^N$
C_{0C1}^N	0	$4A_1^N$
S_{3C1}^N	$4A_2^N$	0
S_{2C1}^N	$4A_3^N$	0
S_{1C1}^N	$20A_2^N$	0

Table XIV: This table contains the Newtonian value of all relevant $a_l^{C_F}$, $a_l^{S_F}$, $b_l^{C_F}$, and $b_l^{S_F}$ coefficients needed for evaluating every nonzero C_F^N and S_F^N in Eq.(43). The left table contains the coefficients for h^{N+} , and in the right one the coefficients for $h^{N\times}$ can be found.

For open orbits there are no difficulties when evaluating series expansion, in the final formulae there are two different types of terms: one contains higher harmonics of the true anomaly parameter, but there are also terms $\sim \chi \cos k\chi/\chi \sin k\chi$. In Table XXIV the coefficients $C_{k\chi}$ and $S_{k\chi}$ of these terms are presented.

-
- [1] LIGO Project, <http://www.ligo.caltech.edu>
 - [2] VIRGO Project, <http://www.virgo.infn.it>
 - [3] GEO600 Project, <http://www.geo600.uni-hannover.de>
 - [4] TAMA Project, <http://tamago.mtk.nao.ac.jp>
 - [5] L. Blanchet, Living Rev. Relativity **9**, 4 (2006).
 - [6] M. Walker and C. M. Will, Phys. Rev. D **19**, 3483 (1979).
 - [7] R. M. O’Leary, B. Kocsis, and A. Loeb, MNRAS **395**, 2127 (2009).
 - [8] K. Danzmann and A. Rüdiger, Classical Quantum Gravity **20**, S1 (2003).
 - [9] L. Barack and C. Cutler, Phys. Rev. D **69**, 082005 (2004).
 - [10] J. M. Weisberg and J. H. Taylor, ASP Conf. Series **328**, 25 (2005).
 - [11] M. Burgay *et al.*, Nature **426**, 531 (2003).
 - [12] B. Willems, V. Kalogera, and M. Henninger, Astrophys. J. **616**, 414 (2004).
 - [13] T. Damour and N. Deruelle, Ann. Inst. Henri Poincaré A **43**, 107 (1985).
 - [14] T. Damour and G. Schäfer, Il Nuovo Cimento B **101**, 127 (1988).
 - [15] R. Rieth and G. Schäfer, Class. Quantum Grav. **14**, 2357 (1997).
 - [16] A. Gopakumar and B. R. Iyer, Phys. Rev. D **56**, 7708 (1997).
 - [17] K. G. Arun, L. Blanchet, B. R. Iyer, and M. S. S. Qusailah, Phys. Rev. D **77**, 064035 (2008).
 - [18] K. G. Arun, L. Blanchet, B. R. Iyer, and S. Sinha, Phys. Rev. D **80**, 124018 (2009).
 - [19] Y. Itoh, Phys. Rev. D **80**, 124003 (2009).
 - [20] M. Tessmer and G. Schäfer, arXiv:1006.3714 [gr-qc]
 - [21] R. O. Hansen, Phys. Rev. D **5**, 1021 (1972).
 - [22] P. C. Peters and J. Mathews, Phys. Rev. **131**, 435 (1963); P. C. Peters, Phys. Rev. **136**, B1224 (1964).
 - [23] M. Turner, Astrophys. J. **216**, 610 (1977).
 - [24] S. J. Kovács and K. S. Thorne, Astrophys. J. **217**, 252 (1977).
 - [25] S. Capozziello, M. de Laurentis, F. de Paolis, G. Ingrosso, and A. Nucita, Mod. Phys. Lett. A **23**, 99 (2008).
 - [26] K. Gültekin, M. C. Miller, and D. P. Hamilton, Astrophys. J. **640**, 156 (2006).
 - [27] K. Martel, Phys. Rev. D **69**, 044025 (1995).
 - [28] J. Majár and M. Vasúth, Phys. Rev. D **77**, 104005 (2008).
 - [29] Z. Keresztes, B. Mikóczi, and L. Á. Gergely, Phys. Rev. D **72**, 104022 (2005).

Harmonic	$\cos [3\Upsilon_0]$	$\cos [\Upsilon_0]$	$\sin [3\Upsilon_0]$	$\sin [\Upsilon_0]$
$C_{6S3}^{0.5+}$	$-4A_1^{0.5}$	0	$A_1^{0.5}$	0
$C_{5S3}^{0.5+}$	$-12A_2^{0.5}$	0	$-A_2^{0.5}$	0
$C_{4S3}^{0.5+}$	$-12(A_1^{0.5} + A_3^{0.5})$	$4A_1^{0.5}$	$-11A_1^{0.5} + 2A_3^{0.5}$	$11A_1^{0.5}$
$C_{3S3}^{0.5+}$	$-4(6A_2^{0.5} + A_4^{0.5})$	$12A_2^{0.5}$	$-5(2A_2^{0.5} - A_4^{0.5})$	$23A_2^{0.5}$
$C_{2S3}^{0.5+}$	$-12(A_1^{0.5} + A_3^{0.5})$	$4(4A_1^{0.5} + 3A_3^{0.5})$	$-13A_1^{0.5} + 14A_3^{0.5}$	$2(28A_1^{0.5} + 11A_3^{0.5})$
$C_{1S3}^{0.5+}$	$-12A_2^{0.5}$	$4(9A_2^{0.5} + A_4^{0.5})$	$15A_2^{0.5}$	$77A_2^{0.5} + 13A_4^{0.5}$
$C_{0S3}^{0.5+}$	$-4A_1^{0.5}$	$12(A_1^{0.5} + A_3^{0.5})$	$7A_1^{0.5}$	$A_1^{0.5} + 42A_3^{0.5}$
$C_{6S1}^{0.5+}$	$-20A_1^{0.5}$	0	$5A_1^{0.5}$	0
$C_{5S1}^{0.5+}$	$-60A_2^{0.5}$	0	$-5A_2^{0.5}$	0
$C_{4S1}^{0.5+}$	$-60(A_1^{0.5} + A_3^{0.5})$	$20A_1^{0.5}$	$5(-11A_1^{0.5} + 2A_3^{0.5})$	$-25A_1^{0.5}$
$C_{3S1}^{0.5+}$	$-20(6A_2^{0.5} + A_4^{0.5})$	$60A_2^{0.5}$	$-25(2A_2^{0.5} - A_4^{0.5})$	$-29A_2^{0.5}$
$C_{2S1}^{0.5+}$	$-60(A_1^{0.5} + A_3^{0.5})$	$20(4A_1^{0.5} + 3A_3^{0.5})$	$-5(13A_1^{0.5} - 14A_3^{0.5})$	$2(-6A_1^{0.5} + 7A_3^{0.5})$
$C_{1S1}^{0.5+}$	$-60A_2^{0.5}$	$20(9A_2^{0.5} + A_4^{0.5})$	$75A_2^{0.5}$	$81A_2^{0.5} + 17A_4^{0.5}$
$C_{0S1}^{0.5+}$	$-20A_1^{0.5}$	$60(A_1^{0.5} + A_3^{0.5})$	$7A_1^{0.5}$	$21A_1^{0.5} + 50A_3^{0.5}$
$S_{6S3}^{0.5+}$	$A_1^{0.5}$	0	$4A_1^{0.5}$	0
$S_{5S3}^{0.5+}$	$-A_2^{0.5}$	0	$12A_2^{0.5}$	0
$S_{4S3}^{0.5+}$	$-11A_1^{0.5} + 2A_3^{0.5}$	$11A_1^{0.5}$	$12(A_1^{0.5} + A_3^{0.5})$	$-4A_1^{0.5}$
$S_{3S3}^{0.5+}$	$-5(2A_2^{0.5} - A_4^{0.5})$	$23A_2^{0.5}$	$4(6A_2^{0.5} + A_4^{0.5})$	$-12A_2^{0.5}$
$S_{2S3}^{0.5+}$	$(-13A_1^{0.5} + 14A_3^{0.5})$	$2(5A_1^{0.5} + 11A_3^{0.5})$	$12(A_1^{0.5} + A_3^{0.5})$	$-4(2A_1^{0.5} + 3A_3^{0.5})$
$S_{1S3}^{0.5+}$	$15A_2^{0.5}$	$A_2^{0.5} + 13A_4^{0.5}$	$12A_2^{0.5}$	$-4(3A_2^{0.5} + A_4^{0.5})$
$S_{6S1}^{0.5+}$	$5A_1^{0.5}$	0	$20A_1^{0.5}$	0
$S_{5S1}^{0.5+}$	$-5A_2^{0.5}$	0	$60A_2^{0.5}$	0
$S_{4S1}^{0.5+}$	$-5(11A_1^{0.5} - 2A_3^{0.5})$	$-25A_1^{0.5}$	$60(A_1^{0.5} + A_3^{0.5})$	$-20A_1^{0.5}$
$S_{3S1}^{0.5+}$	$-25(2A_2^{0.5} - A_4^{0.5})$	$-29A_2^{0.5}$	$20(6A_2^{0.5} + A_4^{0.5})$	$-60A_2^{0.5}$
$S_{2S1}^{0.5+}$	$5(-13A_1^{0.5} + 14A_3^{0.5})$	$2(-23A_1^{0.5} + 7A_3^{0.5})$	$60(A_1^{0.5} + A_3^{0.5})$	$-20(2A_1^{0.5} + 3A_3^{0.5})$
$S_{1S1}^{0.5+}$	$75A_2^{0.5}$	$-21A_2^{0.5} + 17A_4^{0.5}$	$60A_2^{0.5}$	$-20(3A_2^{0.5} + A_4^{0.5})$

Table XV: This table contains the relevant a_i^{CF} , a_i^{SF} , b_i^{CF} , and b_i^{SF} coefficients for evaluating the explicit form of $h^{0.5+}$ in Eq.(44).

[30] L. E. Kidder, Phys. Rev. D **52**, 821 (1995).

[31] C. M. Will and A. G. Wiseman, Phys. Rev. D **54**, 4813 (1996).

Harmonic	$\cos [3\Upsilon_0]$	$\cos [\Upsilon_0]$	$\sin [3\Upsilon_0]$	$\sin [\Upsilon_0]$
$C_{6S2}^{0.5\times}$	$-4A_1^{0.5}$	0	$-16A_1^{0.5}$	0
$C_{5S2}^{0.5\times}$	$4A_2^{0.5}$	0	$-48A_2^{0.5}$	0
$C_{4S2}^{0.5\times}$	$4(11A_1^{0.5} - 2A_3^{0.5})$	$-4A_1^{0.5}$	$-48(A_1^{0.5} + A_3^{0.5})$	$16A_1^{0.5}$
$C_{3S2}^{0.5\times}$	$20(2A_2^{0.5} - A_4^{0.5})$	$-20A_2^{0.5}$	$-16(6A_2^{0.5} + A_4^{0.5})$	$48A_2^{0.5}$
$C_{2S2}^{0.5\times}$	$4(13A_1^{0.5} - 14A_3^{0.5})$	$-8(6A_1^{0.5} + 5A_3^{0.5})$	$-48(A_1^{0.5} + A_3^{0.5})$	$16(4A_1^{0.5} + 3A_3^{0.5})$
$C_{1S2}^{0.5\times}$	$-60A_2^{0.5}$	$-4(39A_2^{0.5} + 7A_4^{0.5})$	$-48A_2^{0.5}$	$16(9A_2^{0.5} + A_4^{0.5})$
$C_{0S2}^{0.5\times}$	$-28A_1^{0.5}$	$-4(3A_1^{0.5} + 22A_3^{0.5})$	$-16A_1^{0.5}$	$48(A_1^{0.5} + A_3^{0.5})$
$S_{6S2}^{0.5\times}$	$-16A_1^{0.5}$	0	$4A_1^{0.5}$	0
$S_{5S2}^{0.5\times}$	$-48A_2^{0.5}$	0	$-4A_2^{0.5}$	0
$S_{4S2}^{0.5\times}$	$-48(A_1^{0.5} + A_3^{0.5})$	$16A_1^{0.5}$	$4(-11A_1^{0.5} + 2A_3^{0.5})$	$4A_1^{0.5}$
$S_{3S2}^{0.5\times}$	$-16(6A_2^{0.5} + A_4^{0.5})$	$48A_2^{0.5}$	$-20(2A_2^{0.5} - A_4^{0.5})$	$20A_2^{0.5}$
$S_{2S2}^{0.5\times}$	$-48(A_1^{0.5} + A_3^{0.5})$	$16(2A_1^{0.5} + 3A_3^{0.5})$	$4(-13A_1^{0.5} + 14A_3^{0.5})$	$-8(A_1^{0.5} - 5A_3^{0.5})$
$S_{1S2}^{0.5\times}$	$-48A_2^{0.5}$	$16(3A_2^{0.5} + A_4^{0.5})$	$60A_2^{0.5}$	$4(-3A_2^{0.5} + 7A_4^{0.5})$

Table XVI: This table contains the relevant $a_i^{C_F}$, $a_i^{S_F}$, $b_i^{C_F}$, and $b_i^{S_F}$ coefficients for evaluating the explicit form of $h^{0.5\times}$ in Eq.(44).

Harmonic	$\cos [4\Upsilon_0]$	$\cos [2\Upsilon_0]$	1
C_{7C4}^{1+}	$15K A_2^1$	0	0
C_{6C4}^{1+}	$35K A_3^1$	0	0
C_{5C4}^{1+}	$81K A_2^1 + 452K A_4^1$	$-24K A_2^1$	0
C_{4C4}^{1+}	$142K A_3^1 + 8K A_5^1$	$-40K A_3^1$	0
C_{3C4}^{1+}	$189K A_2^1 + 1076K A_4^1$	$-144K A_2^1 - 256K A_4^1$	$30K A_2^1$
C_{2C4}^{1+}	$215K A_3^1$	$-152K A_3^1 + 2K A_5^1$	$30K A_3^1$
C_{1C4}^{1+}	$315K A_2^1$	$-504K A_2^1 + 224K A_4^1$	$234K A_2^1 - 24K A_4^1$
C_{0C4}^{1+}	$K A_1^1$	$-4K A_1^1 + 32K A_3^1$	$3K A_1^1 - 6K A_3^1$
C_{7C2}^{1+}	$60K A_2^1$	0	0
C_{6C2}^{1+}	$140K A_3^1$	0	0
C_{5C2}^{1+}	$324K A_2^1 + 1808K A_4^1$	$96(2 - 9\eta)A_2^1$	0
C_{4C2}^{1+}	$568K A_3^1 + 32K A_5^1$	$8(4 - 123\eta)A_3^1$	0
C_{3C2}^{1+}	$756K A_2^1 + 4304K A_4^1$	$96(5 - 14\eta)A_2^1 - 64(13 + 114\eta)A_4^1$	$24(29 - 15\eta)A_2^1$
C_{2C2}^{1+}	$860K A_3^1$	$16(34 - 123\eta)A_3^1 - 8(2 + 9\eta)A_5^1$	$120(1 + 3\eta)A_3^1$
C_{1C2}^{1+}	$1260K A_2^1$	$96(33 - 61\eta)A_2^1 + 64(29 - 120\eta)A_4^1$	$24(235\eta - 33)A_2^1 - 96(37 - 35\eta)A_4^1$
C_{0C2}^{1+}	$4K A_1^1$	$8K A_1^1 + 8(100 - 171\eta)A_3^1$	$-12K A_1^1 - 24(13 - 49\eta)A_3^1 - 12(3 - \eta)A_5^1$
C_{70}^{1+}	$-75K A_2^1$	0	0
C_{60}^{1+}	$-175K A_3^1$	0	0
C_{50}^{1+}	$405K A_2^1 + 2260K A_4^1$	$24(1 - 39\eta)A_2^1$	0
C_{40}^{1+}	$-710K A_3^1 - 40K A_5^1$	$-8(103 + 24\eta)A_3^1$	0
C_{30}^{1+}	$-945K A_2^1 - 5380K A_4^1$	$48(39\eta - 11)A_2^1 - 64(167 - 42\eta)A_4^1$	$6(75\eta - 121)A_2^1$
C_{20}^{1+}	$-1075K A_3^1$	$8(69\eta - 65)A_3^1 - 2(73 - 39\eta)A_5^1$	$-30(5 + 9\eta)A_3^1$
C_{10}^{1+}	$-1575K A_2^1$	$72(91 - 121\eta)A_2^1 - 32(145 - 237\eta)A_4^1$	$6(93 - 823\eta)A_2^1 + 24(149 - 143\eta)A_4^1$
C_{00}^{1+}	$-5K A_1^1$	$32K A_1^1 + 8(128 + 3\eta)A_3^1$	$9K A_1^1 + 6(53 - 199\eta)A_3^1 + 12(3 - \eta)A_5^1$

Table XVII: This table contains all relevant coefficients for evaluating every C_F in Eq.(45) for h^{1+} .

Harmonic	$\sin [4\Upsilon_0]$	$\sin [2\Upsilon_0]$
S_{7C4}^{1+}	$-15K A_2^1$	0
S_{6C4}^{1+}	$-35K A_3^1$	0
S_{5C4}^{1+}	$-81K A_2^1 - 452K A_4^1$	$24K A_2^1$
S_{4C4}^{1+}	$-142K A_3^1 - 8K A_5^1$	$40K A_3^1$
S_{3C4}^{1+}	$-189K A_2^1 - 1076K A_4^1$	$144K A_2^1 + 256K A_4^1$
S_{2C4}^{1+}	$-215K A_3^1$	$152K A_3^1 - 2K A_5^1$
S_{1C4}^{1+}	$-315K A_2^1$	$504K A_2^1 - 224K A_4^1$
S_{7C2}^{1+}	$-60K A_2^1$	0
S_{6C2}^{1+}	$-140K A_3^1$	0
S_{5C2}^{1+}	$-324K A_2^1 - 1808K A_4^1$	$96(9\eta - 2)A_2^1$
S_{4C2}^{1+}	$-568K A_3^1 - 32K A_5^1$	$8(123\eta - 4)A_3^1$
S_{3C2}^{1+}	$-756K A_2^1 - 4304K A_4^1$	$96(14\eta - 5)A_2^1 + 64(13 + 114\eta)A_4^1$
S_{2C2}^{1+}	$-860K A_3^1$	$16(123\eta - 34)A_3^1 + 8(2 + 9\eta)A_5^1$
S_{1C2}^{1+}	$-1260K A_2^1$	$32(87\eta - 33)A_2^1 - 64(29 - 120\eta)A_4^1$
S_{70}^{1+}	$75K A_2^1$	0
S_{60}^{1+}	$175K A_3^1$	0
S_{50}^{1+}	$-405K A_2^1 - 2260K A_4^1$	$24(39\eta - 1)A_2^1$
S_{40}^{1+}	$710K A_3^1 + 40K A_5^1$	$8(103 + 24\eta)A_3^1$
S_{30}^{1+}	$945K A_2^1 + 5380K A_4^1$	$48(11 - 39\eta)A_2^1 + 64(167 - 42\eta)A_4^1$
S_{20}^{1+}	$1075K A_3^1$	$8(65 - 69\eta)A_3^1 + 2(73 - 39\eta)A_5^1$
S_{10}^{1+}	$1575K A_2^1$	$24(219\eta - 89)A_2^1 + (145 - 237\eta)32A_4^1$

Table XVIII: This table contains all relevant coefficients for evaluating every S_F in Eq.(45) for h^{1+} .

Harmonic	$\sin [4\Upsilon_0]$	$\sin [2\Upsilon_0]$
$C_{7C3}^{1\times}$	$60K A_2^1$	0
$C_{6C3}^{1\times}$	$140K A_3^1$	0
$C_{5C3}^{1\times}$	$324K A_2^1 + 1808K A_4^1$	$24K A_2^1$
$C_{4C3}^{1\times}$	$568K A_3^1 + 32K A_5^1$	$40K A_3^1$
$C_{3C3}^{1\times}$	$756K A_2^1 + 4304K A_4^1$	$-24K A_2^1 + 544K A_4^1$
$C_{2C3}^{1\times}$	$860K A_3^1$	$-16K A_3^1 + 16K A_5^1$
$C_{1C3}^{1\times}$	$1260K A_2^1$	$-576K A_2^1 + 1696K A_4^1$
$C_{0C3}^{1\times}$	$4K A_1^1$	$-8K A_1^1 + 232K A_3^1$
$C_{7C1}^{1\times}$	$-60K A_2^1$	0
$C_{6C1}^{1\times}$	$-140K A_3^1$	0
$C_{5C1}^{1\times}$	$-324K A_2^1 - 1808K A_4^1$	$24(7 - 69\eta)A_2^1$
$C_{4C1}^{1\times}$	$-568K A_3^1 - 32K A_5^1$	$-8(109 + 117\eta)A_3^1$
$C_{3C1}^{1\times}$	$-756K A_2^1 - 4304K A_4^1$	$24(37\eta - 7)A_2^1 - 32(385 + 69\eta)A_4^1$
$C_{2C1}^{1\times}$	$-860K A_3^1$	$-112(1 + 9\eta)A_3^1 - 16(11 - 3\eta)A_5^1$
$C_{1C1}^{1\times}$	$-1260K A_2^1$	$192(51 - 77\eta)A_2^1 - 32(133 - 135\eta)A_4^1$
$C_{0C1}^{1\times}$	$-4K A_1^1$	$40K A_1^1 + 8(203 - 93\eta)A_3^1$

Table XIX: This table contains all relevant coefficients for evaluating every C_F in Eq.(45) for $h^{1\times}$.

Harmonic	$\cos [4\Upsilon_0]$	$\cos [2\Upsilon_0]$	1
$S_{7C3}^{1\times}$	$60KA_2^1$	0	0
$S_{6C3}^{1\times}$	$140KA_3^1$	0	0
$S_{5C3}^{1\times}$	$324KA_2^1 + 1808KA_4^1$	$24KA_2^1$	0
$S_{4C3}^{1\times}$	$568KA_3^1 + 32KA_5^1$	$40KA_3^1$	0
$S_{3C3}^{1\times}$	$756KA_2^1 + 4304KA_4^1$	$-24KA_2^1 + 544KA_4^1$	$-48KA_2^1$
$S_{2C3}^{1\times}$	$860KA_3^1$	$-16KA_3^1 + 16KA_5^1$	$-48KA_3^1$
$S_{1C3}^{1\times}$	$1260KA_2^1$	$-816KA_2^1 + 1696KA_4^1$	$-48KA_2^1 - 192KA_4^1$
$S_{7C1}^{1\times}$	$-60KA_2^1$	0	0
$S_{6C1}^{1\times}$	$-140KA_3^1$	0	0
$S_{5C1}^{1\times}$	$-324KA_2^1 - 1808KA_4^1$	$24(7 - 69\eta)A_2^1$	0
$S_{4C1}^{1\times}$	$-568KA_3^1 - 32KA_5^1$	$-8(109 + 117\eta)A_3^1$	0
$S_{3C1}^{1\times}$	$-756KA_2^1 - 4304KA_4^1$	$24(37\eta - 7)A_2^1 - 32(385 + 69\eta)A_4^1$	$48KA_2^1$
$S_{2C1}^{1\times}$	$-860KA_3^1$	$-112(1 + 9\eta)A_3^1 - 16(11 - 3\eta)A_5^1$	$48KA_3^1$
$S_{1C1}^{1\times}$	$1260KA_2^1$	$48(73 - 187\eta)A_2^1 - 32(133 - 135\eta)A_4^1$	$48KA_2^1 + 192KA_4^1$

Table XX: This table contains all relevant coefficients for evaluating every S_F in Eq.(45) for $h^{1\times}$.

Harmonic	$\cos [2\Upsilon_0]$	$\sin [2\Upsilon_0]$	1
C_{4C2}^{N+}	$-BA_5^N$	0	0
C_{3C2}^{N+}	$-(31 + 13\eta)A_{10}^N - 4(10 - 9\eta)A_{11}^N - 2(14 - 17\eta)A_{12}^N$	0	$2(2 - \eta)A_4^N$
C_{2C2}^{N+}	$2(-3 + 5\eta)A_5^N - 10KA_9^N$	$-4BA_5^N$	$4(5 - 4\eta)A_5^N + 28(1 - \eta)A_9^N$
C_{1C2}^{N+}	$(89\eta - 83)A_{10}^N - (48 - 55\eta)A_{11}^N - 2(22 - 31\eta)A_{12}^N$	$-2BA_4^N$	$2(43 - 49\eta)A_{10}^N + 4(20 - 17\eta)A_{11}^N + 4(28 - 25\eta)A_{12}^N$
C_{0C2}^{N+}	$-12KA_1^1 - (28 - 15\eta)A_5^N - (17 - 29\eta)A_9^N$	0	$12KA_1^1 + 3(9 - 5\eta)A_5^N + (33 - 31\eta)A_9^N$
C_{40}^{N+}	$-3BA_5^N$	0	0
C_{30}^{N+}	$-3(31 + 13\eta)A_{10}^N - 12(10 - 9\eta)A_{11}^N - 6(14 - 17\eta)A_{12}^N$	0	$2(\eta - 2)A_4^N$
C_{20}^{N+}	$6(5\eta - 3)A_5^N - 30KA_9^N$	$-12BA_5^N$	$4(4\eta - 5)A_5^N - 28(1 - \eta)A_9^N$
C_{10}^{N+}	$3(89\eta - 83)A_{10}^N - 3(48 - 55\eta)A_{11}^N - 6(22 - 31\eta)A_{12}^N$	$-6BA_4^N$	$2(49\eta - 43)A_{10}^N - 4(20 - 17\eta)A_{11}^N - 4(28 - 25\eta)A_{12}^N$
C_{00}^{N+}	$-36KA_1^1 - 3(28 - 15\eta)A_5^N - 3(17 - 29\eta)A_9^N$	0	$-12KA_1^1 - 3(9 - 5\eta)A_5^N - (33 - 31\eta)A_9^N$

Table XXI: 1PN coefficients for h^{N+} in Eq.(43) from the 1PN description of the motion. This table contains only the 1PN corrections to the coefficients needed to evaluate the C_F^N quantities.

Harmonic	$\cos [2\Upsilon_0]$	$\sin [2\Upsilon_0]$	1
S_{4C2}^{N+}	0	BA_5^N	0
S_{3C2}^{N+}	0	$(31 + 13\eta)A_{10}^N + 4(10 - 9\eta)A_{11}^N + 2(14 - 17\eta)A_{12}^N$	0
S_{2C2}^{N+}	$-4BA_5^N$	$2(3 - 5\eta)A_5^N + 10KA_9^N$	0
S_{1C2}^{N+}	$-2BA_4^N$	$(83 - 89\eta)A_{10}^N + (48 - 55\eta)A_{11}^N + 2(22 - 31\eta)A_{12}^N$	$-2BA_4^N$
S_{40}^{N+}	0	$3BA_5^N$	0
S_{30}^{N+}	0	$3(31 + 13\eta)A_{10}^N + 12(10 - 9\eta)A_{11}^N + 6(14 - 17\eta)A_{12}^N$	0
S_{20}^{N+}	$-12BA_5^N$	$6(3 - 5\eta)A_5^N + 30KA_9^N$	0
S_{10}^{N+}	$-6BA_4^N$	$3(83 - 89\eta)A_{10}^N + 3(48 - 55\eta)A_{11}^N + 6(22 - 31\eta)A_{12}^N$	$6BA_4^N$

Table XXII: 1PN coefficients for h^{N+} in Eq.(43) from the 1PN description of the motion. This table contains only the 1PN corrections to the coefficients needed to evaluate the S_F^N quantities.

Harmonic	$\cos [2\Upsilon_0]$	$\sin [2\Upsilon_0]$
$C_4^{N\times}$	0	$-4BA_5^N$
$C_3^{N\times}$	0	$-4(31 + 13\eta)A_{10}^N - 16(10 - 9\eta)A_{11}^N - 8(14 - 17\eta)A_{12}^N$
$C_2^{N\times}$	$16BA_5^N$	$8(5\eta - 3)A_5^N - 40KA_9^N$
$C_1^{N\times}$	$8BA_4^N$	$4(89\eta - 83)A_{10}^N - 4(48 - 55\eta)A_{11}^N - 8(22 - 31\eta)A_{12}^N$
$C_0^{N\times}$	0	$-16KA_1^N - 12(10 - 9\eta)A_5^N - 4(17 - 23\eta)A_9^N$
$S_4^{N\times}$	$-4BA_5^N$	0
$S_3^{N\times}$	$-4(31 + 13\eta)A_{10}^N - 16(10 - 9\eta)A_{11}^N - 8(14 - 17\eta)A_{12}^N$	0
$S_2^{N\times}$	$8(5\eta - 3)A_5^N - 40KA_9^N$	$-16BA_5^N$
$S_1^{N\times}$	$4(89\eta - 83)A_{10}^N - 4(48 - 55\eta)A_{11}^N - 8(22 - 31\eta)A_{12}^N$	$-8BA_4^N$

Table XXIII: 1PN coefficients for $h^{N\times}$ in Eq.(43) from the 1PN description of the motion.

State	+				×	
	$\cos [2\gamma]$		1		$\cos [\gamma]$	
Υ_0 -harmonic	$\cos [2\Upsilon_0]$	$\sin [2\Upsilon_0]$	$\cos [2\Upsilon_0]$	$\sin [2\Upsilon_0]$	$\cos [2\Upsilon_0]$	$\sin [2\Upsilon_0]$
$C_{3\chi}$	0	$3A_6^N$	0	$9A_6^N$	$-12A_6^N$	0
$C_{2\chi}$	0	$48A_9^N$	0	$144A_9^N$	$-192A_9^N$	0
$C_{1\chi}$	0	$15A_6^N$	0	$45A_6^N$	$-60A_6^N$	0
$C_{0\chi}$	0	$24A_5^N$	0	$72A_5^N$	$-96A_5^N$	0
$S_{3\chi}$	$3A_6^N$	0	$9A_6^N$	0	0	$12A_6^N$
$S_{2\chi}$	$48A_9^N$	0	$144A_9^N$	0	0	$192A_9^N$
$S_{1\chi}$	$15A_6^N$	0	$45A_6^N$	0	0	$60A_6^N$

Table XXIV: This table contains the 1PN coefficients for both polarization states of Eq.(43) from the 1PN description of the motion which are multiplied by χ . The column under the sign "+" contains the coefficients for h^{N+} , and under the sign "×" the coefficients for $h^{N\times}$ can be found.